Development of formalisms based on locally coupled open subsystems for calculations in molecular electronic structure and dynamics

Martín A. Mosquera, Leighton O. Jones, Mark A. Ratner, and George C. Schatz*
Department of Chemistry, Northwestern University, 2145 Sheridan Road, Evanston, Illinois 60208, USA

(Received 29 August 2018; published 5 December 2018)

Quantum embedding theories model a collection of interacting molecules as a set of subsystems, where each can be treated with a particular electronic structure method (wave function or density functional theory, for example); these theories can lead to computationally efficient and accurate algorithms. Motivated by challenges in the field, we previously described a formalism (that models two subsystems), which we call "locally coupled open subsystems" (LCOS), for the computation of ground-state energies, fractional electron-occupation numbers of the subsystems, and the size-consistent limit of subsystem dissociation. In this work we present the full (nonrelativistic) LCOS theory and the following extensions of our previous work: (i) the framework to study systems composed of multiple subsystems and a procedure to spin-adapt the auxiliary wave function that describes the partitioned system, so that its spin state matches that of the real system of interest; (ii) potential functionals and ideas to employ machine learning for the computation of ground-state densities and energies; (iii) formulation of two LCOS ground-state approaches where the fragments are assigned Kohn-Sham wave functions; and (iv) a time-dependent (TD) extension of these two ground-state formalisms in which the state of the subsystems evolves according to a unitary propagation; from this evolution we can extract TD electron populations of the fragments, for instance. We also discuss potential applications of the TD LCOS theory to linear photoabsorption and Raman spectroscopy. The developments presented in this work can lead to ground-state and TD electronic structure calculations where the computational scaling can be controlled, depending on the level of theory and the accuracy desired to model each one of the subsystems and their coupling.

DOI: 10.1103/PhysRevA.98.062505

I. INTRODUCTION

With the aim of computing the electronic ground-state and the dynamical properties of a molecule or solid, dividing it into different subsystems can be advantageous to reduce computational costs and control the level of theory that is convenient to model each subsystem. This strategy allows the user to study systems with a larger size than is traditionally accessible with standard Kohn-Sham density functional theory (DFT) methods. From a computational point of view, algorithms that are able to achieve the following are desirable: (i) to perform separate inexpensive density functional or wave function theory calculations to generate individual information about a fragment, and (ii) to gather and process together the information so generated to produce accurate electronic properties. Theoretically, the mentioned steps offer ways to avoid problems often encountered in the application of semilocal or hybrid functionals—for example, the well-known static correlation errors which often predict incorrect fractional electron occupations in the adiabatic dissociation of molecular fragments [1,2].

Previous work in the field has made it possible to perform subsystem-based quantum chemical calculations with a flexible computational scaling. For example, a molecule can be embedded into different environments such as solvents, surfaces, etc. [3–6]. Modeling of mid- and long-range interactions between dimer molecules, each treated as a separate subsystem, has been reported [7,8]. Recently, interest by the community [9–20] has emerged in developing computational methods—especially from a quantum embedding perspective—to describe the evolution of electronic properties as a function of time, which could facilitate studying phenomena like electron and energy transfer, and predicting time-resolved spectroscopic signals of these types of processes.

Current challenges in the field include developing formalisms and computational methodologies to compute correct electronic populations of molecular subsystems in the static correlation [21] and the time-dependent (TD) regimes [22]. These two issues motivate our formalism, which we call "locally coupled open subsystems" (LCOS). We previously described a simpler version of our methodology [23] to model the electronic ground state, and it features (i) an auxiliary wave function, expressed as a linear combination of tensor products of subsystem states; these states are labeled according to the energy level, number of electrons, spin state, and other symmetry labels; (ii) an auxiliary Hamiltonian which is expressed as a sum of free-subsystem Hamiltonians, plus a coupling operator that induces electron transfer between subsystems; this term depends on a local potential that can be estimated using density functional approximations or machine learning approaches. We refer to this object as "coupling potential," and part of this paper concerns its determination.

The electron population numbers in the LCOS theory are determined by tensor-product wave function amplitudes, which come from Hamiltonian matrix diagonalization (in

*g-schatz@northwestern.edu

ground-state calculations) or, as we show in this work, from unitary propagation in the TD case. These amplitudes depend on the energetics of each fragment and the strength of the coupling between them. The proposed formalism satisfies fragment-wise size consistency: If all the fragments are at infinite separation, then the total ground-state energy is the sum of each isolated-fragment energy. For intermolecular energy transfer problems, the time dependency of the tensor-product superpositions can offer information about the evolution of coherences, and their engineering.

The present work generalizes the approach described in Ref. [23], and it is organized as follows: (i) We define the full expansion of the auxiliary wave function that describes the state of the subsystems, and introduce the required quantum mechanical operators. We study an auxiliary, additive spin operator (defined as the sum of subsystem spin operators), and its corresponding eigenstates; these states may be convenient to mimic the true spin state of the real system of electrons. (ii) We introduce three full ground-state frameworks. The first one is based on correlated wave functions, whereas the other two are developed within density functional theory; treatment of degenerate ground states is included in this work. The first DFT approach is presented on the basis of reference single-particle Hamiltonians, and the second one relies on density matrices and energy functionals. Finally, (iii) we introduce the TD extensions of the theoretical methods mentioned in (ii), i.e., evolution equations for the auxiliary wave function of the system, and its electronic density. We discuss simplification of these equations, one-to-one maps between auxiliary local potentials, and TD electronic densities, an example, and potential applications.

II. TENSOR PRODUCTS AND FRAGMENT-SPECIFIC OPERATORS

Our goal is to estimate ground- and excited-state properties of a system of nonrelativistic electrons. The Hamiltonian of the system reads

$$\hat{H} = \hat{T} + \hat{W} + \int d^3\mathbf{r}\hat{\rho}(\mathbf{r})v(\mathbf{r}); \tag{1}$$

here $\hat{T}$ and $\hat{W}$ are the kinetic and electron repulsion energy operators, respectively; $\hat{\rho}(\mathbf{r})$ is the density operator. These operators are assumed to be given in second quantization, so they are applicable to states with any number of electrons. By means of the Levy constrained search, the ground-state energy functional is expressed as

$$E_v[\rho] = (\min_{\Psi\to\rho}\langle\Psi|\hat{T} + \hat{W}|\Psi\rangle) + \int d^3\mathbf{r}\rho(\mathbf{r})v(\mathbf{r}), \tag{2}$$

where the true ground-state energy of the system, in theory, would be computed by minimizing the above functional over densities that integrate to a given number of electrons.

In the LCOS theory we model the molecular system as a set of fragments, where each fragment is assigned a Hamiltonian with similar form to the one shown above. Instead of minimizing the functional E_v, using the procedure shown above or through the related Kohn-Sham scheme, in this work we optimize an alternative, auxiliary energy operator that we discuss in detail later on. This operator is based on a direct sum of subsystem Hamiltonians, and an interaction operator that induces electron and energy transfer between different subsystems. This interaction operator features a local potential that can be found in a self-consistent fashion, so (in principle) the auxiliary wave function yields the exact density of the real system and its energy, through evaluation of a residual energy that derives from the LCOS formalism. In this work, we consider several, different auxiliary energy operators, which lead to a family of different ground-state and time-dependent formalisms. In practice, selecting the most suitable formalism depends on the type of application, level of theory required to model the subsystems (correlated wave function theory, DFT, etc.), and the desired computational scaling, among others.

We define a set of M auxiliary *open* electronic subsystems. A particular configuration of these subsystems is described by a tensor product of the form

$$|\bar{\Psi}\rangle = |\Psi^1\rangle|\Psi^2\rangle\cdots|\Psi^M\rangle; \tag{3}$$

$|\Psi^Y\rangle$ is a wave function describing the state of fragment Y, and indicates its number of electrons. Throughout this work we refer to a wave function with the form above as a TP (tensor product) wave function. Given another TP wave function $|\bar{\Phi}\rangle = |\Phi^1\rangle\cdots|\Phi^M\rangle$, the inner product is defined as $\langle\bar{\Phi}|\bar{\Psi}\rangle = \langle\Phi^1|\Psi^1\rangle\cdots\langle\Phi^M|\Psi^M\rangle$. As customary in Fock space methods, if two kets of the same fragment describe states with different numbers of electrons, then their inner product is zero, for example $\langle\Phi^Y(N-1)|\Psi^Y(N)\rangle = 0$. Furthermore, we introduce the symbol $(\Phi^Y|\bar{\Psi}\rangle$, where Φ^Y is an arbitrary wave function of the Yth subsystem, which represents the reduced TP wave function:

$$(\Phi^Y|\bar{\Psi}\rangle = [\langle\Phi^Y|\Psi^Y\rangle]|\Psi^1\rangle\cdots[\text{no }|\Psi^Y\rangle]\cdots|\Psi^M\rangle; \tag{4}$$

$(\Phi^Y|\bar{\Psi}\rangle$ is a TP wave function representing $M-1$ fragments.

Each fragment can have any allowed number of electrons; only the total number of electrons remains constant and equals the number of electrons of the real molecule. The ket $|\Psi^Y\rangle$ could be, in principle, the fully correlated wave function of the fragment, or a Slater determinant formed by orbitals that obey the fragment Hartree-Fock equations. Prior to solving these equations, one first specifies the number of electrons in the fragment, the electron-nuclei potential of the Yth fragment, $v_Y(\mathbf{r})$, and the spin symmetry (singlet, doublet, etc.). The Slater determinant can either be pure or spin contaminated.

Multiple ways of dividing a system into different fragments are possible. For example, one can model the molecule as a set of mutually exclusive fragments (that do not share common atoms). Another possibility is the use of overlapping fragments, in which some atoms are shared between different subsystems (this case is advantageous because it can simplify the calculation of embedding potentials significantly). This work, however, focuses on mutually exclusive subsystems, which are assumed given, or preselected (for example, a molecule attached to a nanoparticle might be conveniently partitioned into a nanoparticle subsystem plus the molecule as the other subsystem). A fragment in our theory is represented by its Hamiltonian [Eq. (9) below], which requires a user-defined electron-nuclei potential, for example:

$$v_Y(\mathbf{r}) = \sum_{\alpha\in F_Y} -\frac{Z_\alpha}{|\mathbf{r}-\mathbf{R}_\alpha|}, \tag{5}$$

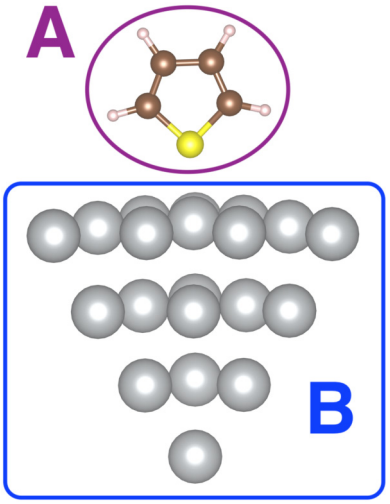

FIG. 1. A thiophene molecule interacting with a Ag_{20} pyramidal cluster. Oval and square shapes surround two possible subsystems, "A" and "B", that the entire system can be partitioned into.

where F_Y is the set of nuclei that are part of fragment Y. In Fig. 1 we show an example of how to divide a thiophene+Ag_{20} composite system. The thiophene domain can be taken as a subsystem, and the pyramidal silver cluster as the other subsystem. In future work we will consider systems like the one shown in Fig. 1.

In this work we employ second-quantized operators. We define a family of annihilation operators $\{\hat{\psi}_Y(\mathbf{r})\}$, where each satisfies

$$\hat{\psi}_Y(\mathbf{r})|\bar{\Psi}\rangle = |\Psi^1\rangle\cdots[\hat{\psi}_Y(\mathbf{r})|\Psi^Y\rangle]\cdots|\Psi^M\rangle; \tag{6}$$

$\hat{\psi}_Y(\mathbf{r})$ and its conjugate only act over the Yth fragment ket. The anticommutation rule of these fragment-specific operators is the same as that of the operator $\hat{\psi}(\mathbf{r})$: $\{\hat{\psi}_Y^\dagger(\mathbf{r}'), \hat{\psi}_Y(\mathbf{r})\} = \delta(\mathbf{r}-\mathbf{r}')$. The density and current density of the Yth fragment can be defined as

$$\hat{\rho}_Y(\mathbf{r}) = \hat{\psi}_Y^\dagger(\mathbf{r})\hat{\psi}_Y(\mathbf{r}),$$
$$\hat{\mathbf{j}}_Y(\mathbf{r}) = \frac{1}{2i}\{\hat{\psi}_Y^\dagger(\mathbf{r})\nabla\hat{\psi}_Y(\mathbf{r}) - [\nabla\hat{\psi}_Y^\dagger(\mathbf{r})]\hat{\psi}_Y(\mathbf{r})\}. \tag{7}$$

Using these quantities, the total density and current density are introduced as the additive operators:

$$\hat{\rho}_+(\mathbf{r}) = \sum_Y \hat{\rho}_Y(\mathbf{r}),\ \hat{\mathbf{j}}_+(\mathbf{r}) = \sum_Y \hat{\mathbf{j}}_Y(\mathbf{r}). \tag{8}$$

The Hamiltonian of fragment Y is defined as follows:

$$\hat{H}_Y = \hat{T}_Y + \hat{W}_Y + \int d^3\mathbf{r}\hat{\rho}_Y(\mathbf{r})v_Y(\mathbf{r}); \tag{9}$$

here $\hat{T}_Y$ and $\hat{W}_Y$ are fragment-specific kinetic and electron repulsion energy operators, respectively. These operators can also be expressed in terms of creation and annihilation operators

$$\hat{T}_Y = \frac{1}{2}\int d^3\mathbf{r}\nabla\hat{\psi}_Y^\dagger(\mathbf{r})\cdot\nabla\hat{\psi}_Y(\mathbf{r}),$$
$$\hat{W}_Y = \int d^3\mathbf{r}d^3\mathbf{r}'\hat{\psi}_Y^\dagger(\mathbf{r}')\hat{\psi}_Y^\dagger(\mathbf{r})\frac{1}{|\mathbf{r}-\mathbf{r}'|}\hat{\psi}_Y(\mathbf{r})\hat{\psi}_Y(\mathbf{r}'). \tag{10}$$

For example, for the state described by Eq. (3), the average energy of fragment Y is $\langle\bar{\Psi}|\hat{H}_Y|\bar{\Psi}\rangle = \langle\Psi^Y|\hat{H}_Y|\Psi^Y\rangle$.

We denote $\Psi^Y_{\mathbf{I}_Y,N_Y}$ as an eigenfunction of the Yth fragment Hamiltonian $\hat{H}_Y$ ($E^Y_{\mathbf{I}_Y,N_Y}|\Psi^Y_{\mathbf{I}_Y,N_Y}\rangle = \hat{H}_Y|\Psi^Y_{\mathbf{I}_Y,N_Y}\rangle$), where N_Y is an integer number of electrons, and the label $\mathbf{I}_Y$ includes the energy level, spin state of the system, and other symmetries. The operator $\hat{\psi}_Y(\mathbf{r})$ can be expressed using a discrete basis: $\hat{\psi}_Y(\mathbf{r}) = \sum_{p\sigma}\psi_{p\sigma,Y}(\mathbf{r})\hat{a}_{p\sigma,Y}$, where $\{\psi_{q\sigma,Y}\}$ are eigenfunctions of some suitable single-particle Hamiltonian (we use the index p for orbital energy level and σ for z spin), and $\hat{a}_{p\sigma,Y}$ destroys an electron occupying $\psi_{p\sigma,Y}$. For example, one can use the eigenfunctions of the Fock operator, $f_{\sigma,Y}$, of the Yth isolated fragment, $f_{\sigma,Y}\psi_{p\sigma,Y} = \epsilon_{p\sigma,Y}\psi_{p\sigma,Y}$.

A. Spin operators

The fragment wave functions can be either closed- or open-shell states. In our model based on subsystems, we introduce a spin operator and a linear combination of tensor products that "mimic" the spin state of the true molecular system. The additive spin operator is the following:

$$\hat{\mathcal{S}} = \hat{\mathbf{S}}_1 + \hat{\mathbf{S}}_2 + \cdots + \hat{\mathbf{S}}_M, \tag{11}$$

where $\hat{\mathbf{S}}_Y$ is the spin (vector) operator of fragment Y [24]. Similarly to $\hat{\psi}_Y$, $\hat{\mathbf{S}}_Y$ only acts over the Yth fragment ket: $\hat{\mathbf{S}}_Y|\bar{\Psi}\rangle = |\Phi_1\rangle\cdots(\hat{\mathbf{S}}_Y|\Phi_Y\rangle)\cdots|\Phi_M\rangle$. Because $\hat{\mathbf{S}}_Y$ and $\hat{\mathbf{S}}_X$ commute if $Y \neq X$, $\hat{\mathcal{S}}$ follows the standard cyclic commutation rule:

$$[\hat{\mathcal{S}}_i, \hat{\mathcal{S}}_j] = i\epsilon_{ijk}\hat{\mathcal{S}}_k, \tag{12}$$

where i, j, and k run over any of the possible Cartesian components (x, y, z). Algebraic procedures, e.g., spin adaption, can be simplified by using raising and lowering operators: $\hat{\mathcal{S}}_+ = \hat{\mathcal{S}}_x + i\hat{\mathcal{S}}_y$ and $\hat{\mathcal{S}}_- = \hat{\mathcal{S}}_x - i\hat{\mathcal{S}}_y$. These operators are related to the additive spin square as follows:

$$\hat{\mathcal{S}}^2 = \hat{\mathcal{S}}_+\hat{\mathcal{S}}_- + \hat{\mathcal{S}}_z(\hat{\mathcal{S}}_z - 1). \tag{13}$$

It can be shown that the raising and lowering operators read $\hat{\mathcal{S}}_+ = \sum_{p,Y}\hat{a}^\dagger_{p\uparrow,Y}\hat{a}_{p\downarrow,Y}$ and $\hat{\mathcal{S}}_- = \sum_{p,Y}\hat{a}^\dagger_{p\downarrow,Y}\hat{a}_{p\uparrow,Y}$.

For a set of open-shell fragments, we could start from a single tensor product configuration, and exchange $\uparrow$ and $\downarrow$ spin states of each singly occupied orbital, while adjusting the sign of the new configuration, to achieve the requested spin symmetry (two doublet fragments can be combined to form a singlet tensor product $\hat{\mathcal{S}}^2|\bar{\Psi}\rangle = 0$ by exchanging the z spin of the outermost orbitals). For example, taking the lithium molecule (Li_2), we can say it is composed of two fragments: a left Li and a right Li atom. The antisymmetrized ket $1/\sqrt{2}(|2s,\uparrow\rangle|2s,\downarrow\rangle - |2s,\downarrow\rangle|2s,\uparrow\rangle)$ (doubly occupied $1s$ levels are omitted) is a singlet eigenstate of $\hat{\mathcal{S}}^2$.

In analogy with standard eigenfunctions of the z-spin and spin-squared operators, we can construct superpositions of TP wave functions such that

$$\hat{\mathcal{S}}^2|\bar{\Psi}\rangle = \mathcal{S}(\mathcal{S}+1)|\bar{\Psi}\rangle, \quad \hat{\mathcal{S}}_z|\bar{\Psi}\rangle = m_{\mathcal{S}}|\bar{\Psi}\rangle. \tag{14}$$

Here $\mathcal{S}$ is a positive integer (1/2, 1, 3/2, etc.) and $m_{\mathcal{S}}$ is a number in the set $(-\mathcal{S}, -\mathcal{S}+1, \ldots, \mathcal{S}-1, \mathcal{S})$.

It is convenient to ensure that given a tensor product of fragment kets, it displays a desired additive-spin symmetry

[Eq. (14)], such as a singlet symmetry, for example. To this end we introduce a spin symmetrization operator, $\mathcal{O}_{\mathscr{S},m_{\mathscr{S}},l_{\mathscr{S}}}$, which, given a set of fragment kets, combines them to produce a linear combination of TP kets that is an eigenfunction of the operators $\hat{\boldsymbol{\mathcal{S}}}^2$ and $\hat{\mathcal{S}}_z$. This operator includes an extra subindex $l_{\mathscr{S}}$ that labels different degenerate states with the same spin numbers $\mathscr{S}$ and $m_{\mathscr{S}}$. We thus write the index $\mathbf{I}_Y$ as $\mathbf{I}_Y = \mathbf{J}_Y m_{\mathrm{S},Y}$ (where $m_{\mathrm{S},Y}$ represents the secondary spin quantum number of fragment Y), and a spin-adapted configuration as

$$\begin{aligned}|\mathbf{J}_1 N_1,\ldots,\mathbf{J}_M N_M;\mathscr{S},m_{\mathscr{S}},l_{\mathscr{S}}\rangle &= \mathcal{O}_{\mathscr{S},m_{\mathscr{S}},l_{\mathscr{S}}}\left|\Psi^1_{\mathbf{J}_1 m_{S,1},N_1}\right\rangle\cdots\left|\Psi^M_{\mathbf{J}_M m_{S,M},N_M}\right\rangle \\ &= \sum_{\mathcal{P}\{m_{S,1},\ldots,m_{S,M}\}} Q_{\mathcal{P}\{m_{S,1},\ldots,m_{S,M}\},\mathscr{S},m_{\mathscr{S}},l_{\mathscr{S}}}\left|\Psi^1_{\mathbf{J}_1\mathcal{P}m_{S,1},N_1}\right\rangle\cdots\left|\Psi^M_{\mathbf{J}_M\mathcal{P}m_{S,M},N_M}\right\rangle, \end{aligned} \tag{15}$$

where $\mathcal{P}$ is an operator that raises the z spin of a fragment and lowers it in another accordingly, and $Q_{\mathcal{P}\{m_{S,1},\ldots,m_{S,M}\},\mathscr{S},m_{\mathscr{S}}}$ is a linear combination coefficient. The above summation is done over all possible spin flips; this step would be dictated by the selected spin-adaption procedure.

To generate configurations that are eigenfunctions of the additive spin operators, one can apply theories based on Löwdin operators, Sanibel coefficients, or related methods. In Appendix B, starting from two triplet states, we apply Löwdin projections to construct a singlet spin-adapted configuration.

B. Electron-transfer coupling and model Hamiltonian

A main aspect of the LCOS theory is the auxiliary Hamiltonian operator. As discussed in Ref. [23], this operator is defined by the following three principles: (i) The Hamiltonian must lead to fragment-wise size consistency. For example, if the system is composed of two fragments, then, as the distance between these fragments tends to infinity, the total energy must tend to the sum of energies of the isolated fragments. (ii) The Hamiltonian must enable control of the computational costs, by allowing the user to select the appropriate level of theory for each fragment, the size of the expansion for the auxiliary wave function, among other settings related to the specific LCOS implementation. Finally, (iii) the model Hamiltonian should include a mechanism that allows for energy and electron transfer among fragments.

Following the above guidelines, we express an auxiliary Hamiltonian as the sum of an additive energy operator and a coupling term. Throughout this work we consider two different additive energy operators: the operator

$$\hat{\mathcal{H}}_+ = \sum_Y \hat{H}_Y, \tag{16}$$

and a similar one expressed in terms of single-particle Hamiltonians, as described in Sec. IV B. A Hamiltonian with the form shown above can satisfy criteria (i) and (ii). To satisfy (ii) one can select different levels of theory, ranging from Hartree-Fock theory, up to full configuration interaction; DFT-based treatment of the fragments is discussed in Sec. IV.

We now consider the term that describes electron transfer. For two subsystems, in Ref. [23] we show that the (local) product of field operators, which eliminates an electron in one fragment and creates a new one in a different fragment, can serve as an electron transfer operator. The generalization of this operator for an arbitrary number of subsystems is straightforward; we define

$$\hat{\zeta}(\mathbf{r}) = \sum_{Y\neq X} \lambda_{YX}\hat{\tau}_{YX}(\mathbf{r}), \tag{17}$$

where $\lambda^*_{XY} = \lambda_{YX}$. The Hermitian matrix $\boldsymbol{\lambda}$ represents the strength of electron-transfer coupling between fragments. In this work we assume this matrix is given. For example, one may choose $\boldsymbol{\lambda}$ as the identity matrix, and find a local auxiliary potential (as required by the formalisms discussed in Sec. III) that describes the electron transfer effects. Alternatively, one can choose a $\boldsymbol{\lambda}$ matrix (different from the identity matrix) such that it simplifies the development of approximations to the auxiliary potential. In a future work we will explore methodologies to compute this matrix. The symbol $\hat{\tau}_{YX}(\mathbf{r})$ represents an operator that annihilates an electron in subsystem X and creates another one in fragment Y, and is defined as

$$\hat{\tau}_{YX}(\mathbf{r}) = \hat{\psi}^\dagger_Y(\mathbf{r})\hat{\psi}_X(\mathbf{r}). \tag{18}$$

This operator satisfies $\hat{\tau}^\dagger_{YX} = \hat{\tau}_{XY}$, which implies that $[\hat{\tau}_{YX}(\mathbf{r}) + \hat{\tau}_{XY}(\mathbf{r})]$ and $\hat{\zeta}(\mathbf{r})$ are Hermitian.

To couple the fragments so energy transfer can take place, we employ the additive density operator $\hat{\rho}_+$. This term, however, is particle conserving, meaning it does not induce charge transfer between subsystems. The net coupling in our theory is thus collected into a single local operator. We refer to it as a "pseudodensity", and it reads

$$\hat{\eta}(\mathbf{r}) = \hat{\rho}_+(\mathbf{r}) + \hat{\zeta}(\mathbf{r}). \tag{19}$$

The strength of this net coupling is controlled by a local auxiliary potential, $\theta(\mathbf{r})$, which can be estimated by employing a density functional, or other techniques such as machine learning. In this work we study auxiliary Hamiltonians (in Ref. [23] we employ the symbol $\hat{\mathcal{H}}$ to represent this Hamiltonian) with the following form:

$$\hat{\mathcal{H}} = \hat{\mathcal{H}}_+ + \int d^3\mathbf{r}\hat{\eta}(\mathbf{r})\theta(\mathbf{r}). \tag{20}$$

Variations of this operator and local potential, introduced as required by each theory, are discussed in the following sections [25].

The type of energy operator shown above fulfills a similar role in our theories to that of the Kohn-Sham Hamiltonian within standard DFT—to provide a convenient set of Schrödinger-like equations that has a lower computational cost than traditional correlated wave function methods—and features a local potential (like the XC potential) that can be estimated through derivation of a density functional (such as

the XC energy). The Kohn-Sham (KS) equations lead to estimation of the ground-state density of the system. Furthermore, the ground-state energy in KS DFT is approximated as usual in terms of the (noninteracting) kinetic, XC, Hartree, and electron-nuclei attraction energies. In a similar fashion, in the LCOS theory we express the electronic ground-state energy of the system as the sum of a known energy and an unknown term that needs to be approximated as a density functional (or as a quantity that could be determined by a machine learning algorithm).

III. GROUND-STATE FORMALISMS

As mentioned in the previous section, we assume that the molecular system is divided into a set of M subsystems. These are taken as auxiliary fragments, where each is associated with a specific set of operators, namely, energy, density, current density, and spin. In addition, we introduce in the following in this section auxiliary local potentials and pairwise operators that account for the coupling between all the fragments, so they exchange charge and energy. The frameworks we discuss, strictly speaking, are designed to calculate the properties of the lowest-energy state with given values of spin numbers S, m_S of the real molecular system.

The present section is organized as follows: First, we present potential functionals that can be used within the context of machine learning to find the correlation between local potentials and densities, and ground-state energies and nuclear coordinates; these correlations could then be used to predict ground-state properties. Second, density functionals are introduced; these allow for computation of the local potential in terms of functional derivatives; the ground-state energy of the system is computed as the additive energy of the subsystems, plus an energy functional that corrects the additive energy. And, third, a simple example is considered, which was reported in detail in Ref. [23].

A. Potential functionals and eigenvalue problem

In previous work, starting from a density functional that we define as a constrained minimization of the additive energy operator, $\hat{\mathcal{H}}_+$, over the space of TP superpositions, we derived eigenvalue equations that, if solved self-consistently, can yield the ground-state density of the system [23]. Once the density is obtained, one then computes the energy as the average of the operator $\hat{\mathcal{H}}_+$, plus a residual energy functional (also referred to as "coupling" energy), which is evaluated at the ground-state density [23]; this topic is discussed in detail in Sec. III C. In this section we show that the eigenvalue equation can be rederived on the basis of a potential functional. We introduce the general ansatz to solve the eigenvalue problem, and reduced density matrices that can be applied for the computation of subsystem energies and densities. In Sec. III B we use one-to-one maps between coupling potentials and pseudodensities, and discuss how potential functionals may be studied with machine learning methods.

The energy potential functional is defined as follows:

$$\mathcal{E}^{\mathrm{MB}}[\theta_{\mathrm{MB}}] = \min_{\bar{\Psi}} \langle \bar{\Psi}|\hat{\mathcal{H}}_+ + \int d^3\mathbf{r}\hat{\eta}(\mathbf{r})\theta_{\mathrm{MB}}(\mathbf{r})|\bar{\Psi}\rangle; \quad (21)$$

here θ_{MB} is an auxiliary local potential. We employ the acronym "MB" to imply that the fragments are described by fully correlated wave functions and many-body (MB) Hamiltonians. We refer to θ_{MB} as the "coupling" potential. Its role is to control the shape of each fragment electronic density, and the amount of charge transferred among fragments. We restrict the search above to superpositions of TP wave functions that have the same spin number as that of the true ground-state wave function of the entire system. For example, if the total system is a doublet state then we demand $\mathscr{S} = S = 1/2$, and $m_{\mathscr{S}} = +1/2$ or $-1/2$.

Even though in this section we express the additive operator $\mathcal{H}_+$ as the sum of *nonrelativistic, all-electron* subsystem Hamiltonians, other choices are possible. In Sec. IV B we discuss an alternative additive energy operator that can serve as the starting point for DFT-based treatment of subsystem electronic states.

The above minimization problem can be solved using an ansatz of the form

$$|\bar{\Psi}\rangle = \sum_{\mathbf{J}_1 N_1,\ldots,\mathbf{J}_M N_M, l_{\mathscr{S}}} C_{\mathbf{J}_1 N_1,\ldots,\mathbf{J}_M N_M, l_{\mathscr{S}}} |\mathbf{J}_1 N_1, \ldots, \mathbf{J}_M N_M; \mathscr{S}, m_{\mathscr{S}}, l_{\mathscr{S}}\rangle, \quad (22)$$

where the summation is performed over electron numbers $\{N_Y\}$ that conserve the total number of electrons ($\sum_Y N_Y = N_{\mathrm{T}}$, where N_{T} is the total number of electrons). For convenience we collect all the indices with a single vector $\bar{\mathbf{J}}$. Therefore we write the above ansatz more compactly as $|\bar{\Psi}\rangle = \sum_{\bar{\mathbf{J}}} C_{\bar{\mathbf{J}}}|\bar{\mathbf{J}}\rangle$. Using the above orthonormal basis [26], Eq. (21) can be expressed, and solved accordingly, as a standard eigenvalue problem:

$$[\boldsymbol{\mathcal{H}}_+ + \boldsymbol{\Theta}_{\mathrm{MB}}]\mathbf{C}^I = E_I \mathbf{C}^I, \quad (23)$$

where $(\boldsymbol{\mathcal{H}}_+)_{\bar{\mathbf{J}}'\bar{\mathbf{J}}} = \langle \bar{\mathbf{J}}'|\hat{\mathcal{H}}_+|\bar{\mathbf{J}}\rangle$ and $(\boldsymbol{\Theta}_{\mathrm{MB}})_{\bar{\mathbf{J}}'\bar{\mathbf{J}}} = \langle \bar{\mathbf{J}}'|\int d^3\mathbf{r}\hat{\eta}(\mathbf{r})\theta_{\mathrm{MB}}(\mathbf{r})|\bar{\mathbf{J}}\rangle$. We denote the ground-state wave function that solves the right-hand side (rhs) of Eq. (21) as $|\bar{\Psi}^0\rangle = \sum_{\bar{\mathbf{J}}} C^0_{\bar{\mathbf{J}}}|\bar{\mathbf{J}}\rangle$. For the calculation of averages such as $\langle \bar{\Psi}^0|\hat{H}_Y|\bar{\Psi}^0\rangle$, we define the reduced density matrix:

$$w^Y_{\mathbf{I}_Y\mathbf{I}'_Y N_Y} = \mathrm{tr}_{X\neq Y}\left\{\left(\Psi^Y_{\mathbf{I}_Y N_Y}|\bar{\Psi}^0\rangle\langle\bar{\Psi}^0|\Psi^Y_{\mathbf{I}'_Y N_Y}\right)\right\}. \quad (24)$$

In this operation we treat all the fragments but the Yth fragment as bath states, and trace them out (Appendix A). Using this matrix we can further introduce the reduced density operator

$$\hat{D}_Y = \sum_{\mathbf{I}_Y\mathbf{I}'_Y N_Y} w^Y_{\mathbf{I}_Y\mathbf{I}'_Y N_Y} \left|\Psi^Y_{\mathbf{I}_Y N_Y}\right\rangle\left\langle\Psi^Y_{\mathbf{I}'_Y N_Y}\right|. \quad (25)$$

Hence the additive energy takes the form

$$\langle\bar{\Psi}^0|\hat{\mathcal{H}}_+|\bar{\Psi}^0\rangle = \sum_Y \mathrm{tr}\{\hat{H}_Y\hat{D}_Y\}; \tag{26}$$

similarly, the additive density of the system reads $\rho_+(\mathbf{r}) = \sum_Y \mathrm{tr}\{\hat{D}_Y\hat{\rho}_Y(\mathbf{r})\}$.

The above expressions imply that one can compute fragment-specific quantities using a density-matrix perspective. However, note that the density matrix $\hat{D}_Y$ does not derive from a physical ensemble model, as in other versions of fragment-based density functional theories such as partition DFT [27] and potential functional embedding DFT [5] (Appendix F), or standard all-electron theories that rely on statistical thermodynamical ensembles [28,29]. We remark that the state of all the fragments is described by the linear combination of TP states $|\bar{\Psi}\rangle$.

B. One-to-one maps and estimation of potentials

We denote the TP wave function that, for a given potential θ_{MB}, minimizes the rhs of Eq. (21) as $\bar{\Psi}_0$. Suppose that for a different coupling potential θ'_{MB} there is a corresponding nondegenerate ground-state TP wave function $\bar{\Psi}'_0$. If these two states are nondegenerate, then they cannot give rise to the same pseudodensity (this result follows the usual *reductio ad absurdum* procedure).

The above theorem thus implies the existence of a functional that associates to a given pseudodensity, η, a unique coupling potential. In contrast with this result, establishing a one-to-one mapping between coupling potentials and total electronic densities is more challenging. For practical applications, however, we assume that each density is assigned a unique coupling potential. If the map is many-to-one, we believe it is possible to add constraints and employ approximations that lead to one-to-one maps between electronic densities and local coupling potentials.

For a given electronic density, machine learning methods might assist in finding a coupling potential that represents such density, and its related coupling energy. By finding a potential that "represents a given density" we refer to determining a potential $\theta_{\mathrm{MB},0}$ with the following property: that the auxiliary wave function that solves the rhs of Eq. (21) with $\theta_{\mathrm{MB},0}$ yields an electronic density that exactly matches the given density. In practice, to find $\theta_{\mathrm{MB},0}$ one can employ a procedure in which a cost function is minimized. Such function would measure the deviation of a density represented by some intermediate coupling potential from the density of interest. Tools such as kernel regression may be employed to represent trial coupling potentials, and to minimize the cost function. Within the context of standard KS theory, the work of Snyder *et al.* [30] presents ideas to employ kernel methods to compute kinetic energy functionals, and perhaps they are applicable to finding coupling energy functionals as well.

C. Deriving coupling potentials and energies from density functionals

We now discuss the application of DFT principles to compute the local coupling potential, and the ground-state energy by means of the additive and the coupling energies, which are defined as density functionals in this subsection. The definitions we present in this section lead to a methodology that can be convenient for numerical simulations, and in which we obtain (among other density-derivable quantities such as dipole moments) electron populations from a wave function that solves an eigenvalue problem.

Regarding the auxiliary Hamiltonian shown in Eq. (20), we note that it has a single local coupling potential which is multiplied by the pseudodensity operator $\hat{\eta}$. This potential is introduced to account for the transfer of energy and charge between subsystems. With the purpose of relating the coupling potential with the functional derivative of an energy term that depends on the electronic density, in this subsection we show that this is achieved by working with the ground-state energy expressed in terms of a double-constrained search functional for the additive energy and a residual energy term, where both depend on the electronic density being estimated. Approximating the residual and additive energies as functionals of the density is convenient because quantities such as the electrostatic and XC energies depend explicitly on the density. The double-constrained search is used in this work because the pseudodensity and the coupling potential are conjugate variables, and an additional search is needed to switch from the regime of pseudodensities to the domain of electronic densities.

On the basis of the existence of one-to-one maps between the space of pseudodensities and coupling potentials, we define the following constrained-search functional:

$$\mathcal{E}_+^{\mathrm{MB}}[\eta] = \min_{\bar{\Psi}}\{\langle\bar{\Psi}|\hat{\mathcal{H}}_+|\bar{\Psi}\rangle|\langle\bar{\Psi}|\hat{\eta}(\mathbf{r})|\bar{\Psi}\rangle = \eta(\mathbf{r})\}. \tag{27}$$

Although this functional is different from $\mathcal{E}^{\mathrm{MB}}$ because they depend on different variables, they are related to one another through a Legendre transformation. Now suppose that the TP ket $|\bar{\Psi}[\eta]\rangle$ solves the above problem, Eq. (27). This object allows us to define the following density functional,

$$E_+^{\mathrm{MB}}[\rho] = \min_{\eta}\{\mathcal{E}_+^{\mathrm{MB}}[\eta]|\eta(\mathbf{r}) - \zeta[\eta](\mathbf{r}) = \rho(\mathbf{r})\}, \tag{28}$$

where $\zeta[\eta](\mathbf{r}) = \langle\bar{\Psi}[\eta]|\hat{\zeta}(\mathbf{r})|\bar{\Psi}[\eta]\rangle$; the constraint on the rhs of the above equation can be written alternatively as $\langle\bar{\Psi}[\eta]|\hat{\rho}_+(\mathbf{r})|\bar{\Psi}[\eta]\rangle = \rho(\mathbf{r})$. Similarly to what we did in the previous section, we formally define the coupling energy functional as follows:

$$B^{\mathrm{MB}}[\rho] = E_v[\rho] - E_+^{\mathrm{MB}}[\rho]. \tag{29}$$

This relation enables us to relate $B^{\mathrm{MB}}[\rho]$ with a coupling potential, as we describe next.

We showed in Ref. [23], supporting information section, that Eq. (28) can be solved using the Lagrange-multiplier method, giving us the coupling potential. For convenience we express it with the symbol $\theta_{\mathrm{MB}}[\eta]$, and as a functional of the pseudodensity η: if η varies, so does $\theta_{\mathrm{MB}}[\eta]$. Note that in Secs. III A and III B the symbol θ_{MB} refers to a potential that is independent of ρ.

For a potential $\theta_{\mathrm{MB}}[\eta]$, one solves a Schrödinger-like eigenvalue problem [Eq. (32) below] to find an auxiliary wave function, with the lowest eigenvalue, that yields the pseudodensity η. Second, we introduce a functional $\tilde{\eta}$ such that, when evaluated at ρ, it solves Eq. (28). This functional then allows us to write $E_+^{\mathrm{MB}}[\rho] = \mathcal{E}_+^{\mathrm{MB}}[\tilde{\eta}[\rho]]$. By means of this nested form and the chain rule, we express the derivative

$\delta E_+^{\rm MB}[\rho]/\delta\rho(\mathbf{r})$ in terms of $\theta_{\rm MB}[\eta]$ as follows:

$$\frac{\delta E_+^{\rm MB}}{\delta\rho(\mathbf{r})} = -\theta_{\rm MB}[\tilde{\eta}[\rho]](\mathbf{r}) - \int d^3\mathbf{r}\frac{\delta\tilde{\zeta}(\mathbf{r}')}{\delta\rho(\mathbf{r})}\theta_{\rm MB}[\tilde{\eta}[\rho]](\mathbf{r}'), \tag{30}$$

where $\tilde{\zeta}(\mathbf{r}') = \langle\bar{\Psi}[\tilde{\eta}[\rho]]|\hat{\zeta}(\mathbf{r})|\bar{\Psi}[\tilde{\eta}[\rho]]\rangle$.

Now we take the functional derivative of $B^{\rm MB}$ by applying the operator $\delta/\delta\rho(\mathbf{r})$ to both sides of Eq. (29), and evaluate the result at the true ground-state density of the system, ρ_0. At this density, ρ_0, the Hohenberg-Kohn principle implies that $\delta E_v[\rho]/\delta\rho(\mathbf{r}) = $ constant. Through this principle and Eq. (30), we derive the following relation between the coupling functional and potential (Ref. [23]):

$$\theta_{\rm MB,0}(\mathbf{r}) + \int d^3\mathbf{r}'\theta_{\rm MB,0}(\mathbf{r}')\frac{\delta\tilde{\zeta}(\mathbf{r}')}{\delta\rho(\mathbf{r})}\bigg|_{\rho=\rho_0} = \frac{\delta B^{\rm MB}}{\delta\rho(\mathbf{r})}\bigg|_{\rho=\rho_0}, \tag{31}$$

where an arbitrary constant is omitted in the above equation, and $\theta_{\rm MB,0} = \theta_{\rm MB}[\rho_0]$. This equation expresses a condition that must be met in order to minimize the ground-state energy functional $E_v[\rho]$, and, simultaneously, obtain the required coupling potential ($\theta_{\rm MB,0}$) that is needed to find the auxiliary function that reproduces the ground-state density ρ_0. This auxiliary wave function is the solution, with lowest eigenvalue, to the equation

$$\left\{\hat{\mathcal{H}}_+ + \int d^3\mathbf{r}\hat{\eta}(\mathbf{r})\theta_{\rm MB,0}(\mathbf{r})\right\}|\bar{\Psi}_I\rangle = E_I|\bar{\Psi}_I\rangle. \tag{32}$$

As in Sec. III A, the above equation can be solved in matrix form: $(\boldsymbol{\mathcal{H}}_+ + \boldsymbol{\Theta})\mathbf{C}_I = E_I\mathbf{C}_I$.

We remark that Eq. (31) is a condition that is met once the ground-state problem has been solved. However, the coupling potential depends on the density, a quantity one does not know beforehand. Motivated by this and by the standard Kohn-Sham DFT method, we can take Eq. (31) as a relation to generate coupling potentials: one guesses a suitable ground-state density, ρ_0', and then solves Eq. (31) (with ρ_0 replaced by ρ_0') to obtain an estimate to $\theta_{\rm MB,0}$ that is fed back into the eigenvalue problem, Eq. (32), to generate a new auxiliary wave function. This wave function can then produce a new estimate of the ground-state density, and the mentioned procedure is repeated again (obtain a new coupling potential, solve the eigenvalue equation, and so on) until differences in density among iterations become negligible. These steps we just described constitute a fixed-point iterative scheme.

The reader may note that Eq. (29) is a formal definition, and it leads to a "chicken-or-the-egg" dilemma. In this vicious cycle we express an undetermined quantity ($\theta_{\rm MB}$) in terms of another undetermined object, $B^{\rm MB}$, which is a functional that depends on the energy functional, which is unknown in analytical form. This dilemma is removed when an approximation to $B^{\rm MB}$ (we assume the matrix $\boldsymbol{\lambda}$ is already given) is introduced and employed to find solution of the (approximate) self-consistent problem. For practical applications, an approximation to $B^{\rm MB}$ would be employed for two purposes: first, to approximate the coupling potential $\theta_{\rm MB,0}$ for a given density, and second, to finally estimate the ground-state energy as

$$E_v[\rho_0'] \approx E_+^{\rm MB}[\rho_0'] + B_{\rm approx}^{\rm MB}[\rho_0']; \tag{33}$$

here ρ_0' is the final approximation to the true ground-state density, $B_{\rm approx}^{\rm MB}$ is the approximation to $B^{\rm MB}$, and $E_+^{\rm MB}$ is evaluated using the auxiliary wave function with lowest eigenvalue, obtained by solving Eq. (32): $E_+^{\rm MB}[\rho_0'] = \langle\bar{\Psi}_0|\hat{\mathcal{H}}_+|\bar{\Psi}_0\rangle$. As we discussed in Ref. [23], the coupling energy has several contributions from different energies: kinetic, XC, Hartree, and electron-nuclei interaction. This decomposition provides pathways to apply standard approximations to estimate $B^{\rm MB}$, as further discussed in Ref. [23].

In principle, an approximation to the coupling energy functional and a reference matrix $\boldsymbol{\lambda}$ are needed prior to finding the ground-state density and energy of the system, through self-consistent solution of Eq. (32) and evaluation of the rhs of Eq. (33). However, for practical calculations, the term $\delta\tilde{\zeta}(\mathbf{r}')/\delta\rho(\mathbf{r})$ may be challenging to implement in computer codes. To avoid this, one can ignore this term as an additional approximation, and estimate the coupling potential simply as

$$\theta_{\rm MB,0}(\mathbf{r}) \approx \frac{\delta B_{\rm approx}^{\rm MB}}{\delta\rho(\mathbf{r})}\bigg|_{\rho=\rho_0'}. \tag{34}$$

Currently, the effect of neglecting $\delta\tilde{\zeta}(\mathbf{r}')/\delta\rho(\mathbf{r})$ is unknown to us. But, we expect that approximations to $B^{\rm MB}$ may absorb this effect and allow for computation of $\theta_{\rm MB}$ as stated in the above equation; our previous study [23] suggests this may be possible. In Sec. IV B, we briefly revisit the topic of relating coupling potentials with energies, within the context of the DFT-treatment of subsystem electronic structure.

D. Example

In previous work (Ref. [23]) we considered an A+B system, with A representing a lithium atom, and B hydrogen. We employed a simple ansatz for the auxiliary wave function, consisting of a linear combination of a neutral and a charge-transfer configuration ($|\mathrm{A}^+\rangle|\mathrm{B}^-\rangle$). The neutral configuration is the tensor product $|\mathrm{A},\uparrow\rangle|\mathrm{B},\downarrow\rangle$, where each ket represents the restricted open-shell Hartree-Fock determinants of systems A and B, respectively (the arrow indicates the z spin of the electron of the highest, half-occupied atomic orbital). This neutral configuration, however, is not an eigenfunction of $\hat{\boldsymbol{\mathcal{S}}}^2$. If we use instead the symmetrized configuration $1/\sqrt{2}(|\mathrm{A},\uparrow\rangle|\mathrm{B},\downarrow\rangle - |\mathrm{A},\downarrow\rangle|\mathrm{B},\uparrow\rangle)$, denoted as $|\mathrm{A},\mathrm{B}\rangle_S$, then the ansatz

$$|\bar{\Psi}\rangle = C_{\rm N}|\mathrm{A},\mathrm{B}\rangle_{\mathcal{S}} + C_{\rm CT}|\mathrm{A}^+\rangle|\mathrm{B}^-\rangle \tag{35}$$

is a singlet state of $\hat{\boldsymbol{\mathcal{S}}}^2$.

Suppose the restricted Hartree-Fock wave functions of A and B are determined using as reference the neutral atomic states and that the determinants for A^+ and B^- are constructed using the orbitals of the corresponding neutral atomic states. Regarding $C_{\rm N}$ and $C_{\rm CT}$ as the variational coefficients, following similar steps to those in Ref. [23], we arrive at the secular equation [which is a truncated form of Eq. (23)]:

$$\begin{pmatrix} 0 & \Theta_{\rm CT,N} \\ \Theta_{\rm CT,N} & I_{\rm A} - A_{\rm B} + \Delta\Theta \end{pmatrix}\begin{pmatrix} C_{\rm N} \\ C_{\rm CT} \end{pmatrix} = \tilde{\mathcal{E}}\begin{pmatrix} C_{\rm N} \\ C_{\rm CT} \end{pmatrix}; \tag{36}$$

here $\tilde{\mathcal{E}}$ is an eigenvalue; $I_{\rm A}$ and $A_{\rm B}$ represent the ionization and the electron affinity potentials of A and B, respectively; $\Delta\Theta$ is the energy shift $\int d^3\mathbf{r}\,\theta_{\rm MB}(\mathbf{r})[\rho_{\rm CT}(\mathbf{r}) - \rho_{\rm N}(\mathbf{r})]$

[where ρ_{CT} and ρ_N are the total densities of the charge-transfer and neutral configurations, and they read $\rho_{CT}(\mathbf{r}) = \langle A^+|\langle B^-|\hat{\rho}_+(\mathbf{r})|A^+\rangle|B^-\rangle$ and $\rho_N(\mathbf{r}) = {}_{\mathcal{S}}\langle A, B|\hat{\rho}_+(\mathbf{r})|A, B\rangle_{\mathcal{S}}$; for convenience we subtract the additive energy of the neutral configuration from the diagonal of the Hamiltonian matrix]; and $\theta_{MB}(\mathbf{r})$ is a coupling potential. The off-diagonal coupling ($\Theta_{CT,N}$) reads [31] $\lambda_{AB}/\sqrt{2}\int d^3\mathbf{r}\theta_{MB}(\mathbf{r})\varphi_{HOMO,A}(\mathbf{r})\varphi_{HOMO,B}(\mathbf{r})$.

In this previous work, for a given Li-H internuclear distance, we applied a density functional to approximate B^{MB}, and decomposed this energy in terms of a modified Thomas-Fermi kinetic energy, an XC local-density approximation, and electrostatic contributions. The local coupling potential was estimated using $\delta B^{MB}/\delta\rho(\mathbf{r})$, and the secular equation was solved self-consistently. Using the coefficients with lowest energy that solve the eigenvalue problem, we can write, for instance, the average number of electrons in subsystem A, $\langle N_A\rangle$, as

$$\langle N_A\rangle = \langle\bar{\Psi}|\int d^3\mathbf{r}\hat{\rho}_A(\mathbf{r})|\bar{\Psi}\rangle = J_A|C_N|^2 + (J_A-1)|C_{CT}|^2, \tag{37}$$

where $J_A = 3$, the number of electrons of Li in its neutral state; in Ref. [23] we further discuss the meaning of averages like $\langle N_A\rangle$, and alternative ways to compute it. We showed that the above approximations lead to fragment occupation numbers that satisfy physical constraints, such as size consistency and their expected behavior around the equilibrium internuclear distance, in which it is known that the configuration $|A^+\rangle|B^-\rangle$ is dominant. Another restriction that is met by the secular equation is that the local potential $\theta_{MB}(\mathbf{r})$ and coupling energy B^{MB} tend to zero as the internuclear distance tends to infinity; this feature leads to size consistency.

IV. SUBSYSTEM DESCRIPTION USING DENSITY FUNCTIONAL THEORY

In this section we discuss two potential extensions of our formalism to treat the subsystems by using principles of DFT. The first extension is an application of the previous MB formalism in which we replace the fully correlated Hamiltonians by reference KS Hamiltonians. In the second extension, we employ density matrices to define different kinds of additive energy functionals that are used to derive a self-consistent eigenvalue problem that solves a minimization problem that involves variations of linear-combination coefficients and subsystem orbitals.

An important point to take into account is that an isolated subsystem may have a set of degenerate ground states, which may not only involve spin, but other degrees of freedom. For this reason, we begin discussing a formulation for such case.

A. Density-matrix formalism of isolated multiplets

To describe a subsystem with a set of degenerate ground states, we employ as an initial point of reference the work of Nagy [32], who showed that averages of density matrices describing states with a given symmetry can be used to define energy density functionals. We begin introducing the following Levy functional for a single system,

$$F[\rho](\mathbf{w}) = \min_{\hat{D}\to\rho}\mathrm{tr}\{(\hat{T}+\hat{W})\hat{D}\}, \tag{38}$$

and the minimization is performed over density matrices of the form

$$\hat{D} = \sum_{N\boldsymbol{\gamma}\boldsymbol{\gamma}'} w_{\boldsymbol{\gamma}\boldsymbol{\gamma}'N}|\Psi_{\boldsymbol{\gamma}N}\rangle\langle\Psi_{\boldsymbol{\gamma}'N}|, \tag{39}$$

where the wave functions are fully correlated and antisymmetrized, and the index $\boldsymbol{\gamma}$ represents a set of degenerate levels (including spin) that are labeled according to the spatial and spin symmetries of the ground state. To minimize the rhs of Eq. (38), only variations of the wave functions are allowed, whereas matrix $\mathbf{w}$ is held fixed.

In Ref. [32], the matrix $\mathbf{w}$ is diagonal, i.e., $w_{\boldsymbol{\gamma}'\boldsymbol{\gamma},N} = \delta_{\boldsymbol{\gamma}'\boldsymbol{\gamma}}\tilde{w}_{\boldsymbol{\gamma},N}$. For the formalism that we introduce in Sec. IV C, we consider $\mathbf{w}$ matrices that have off-diagonal nonzero elements. Following Eq. (25), we note that such matrices are required to compute fragment electronic densities, $\{\rho_Y\}$.

We now introduce the Hartree-exchange-correlation (HXC) potential:

$$E_{HXC}[\rho](\mathbf{w}) = F[\rho](\mathbf{w}) - T_s[\rho](\mathbf{w}), \tag{40}$$

where

$$T_s[\rho](\mathbf{w}) = \min_{\hat{D}_s\to\rho}\mathrm{tr}\{\hat{T}\hat{D}_s\}, \tag{41}$$

and $\hat{D}_s = \sum_{N\boldsymbol{\gamma}\boldsymbol{\gamma}'} w_{\boldsymbol{\gamma}\boldsymbol{\gamma}'N}|\Psi_{s,\boldsymbol{\gamma}N}\rangle\langle\Psi_{s,\boldsymbol{\gamma}'N}|$. The wave functions $\{\Psi_{s,\boldsymbol{\gamma}N}\}$ are linear combinations of Slater determinants, which are constructed by means of a single orthonormal orbital basis. For example, when orbital degeneracies are present one can use the Löwdin method to transform a reference determinant into a combination of more Slater determinants, so the required J and M_J eigenvalues are obtained. This method reduces to the usual KS-DFT scheme when degeneracies are absent or only involve spin multiplets.

To calculate the HXC potential, we only need the density and the matrix $\mathbf{w}$. This potential is expressed in a manner similar to that in standard KS theory:

$$v_{HXC}(\mathbf{r}) = \frac{\delta E_{HXC}}{\delta\rho(\mathbf{r})}. \tag{42}$$

Note, however, that the HXC energy functional defined by Eq. (40) is, by definition, different from the standard HXC functional used in standard KS DFT, namely, LDA, GGA, etc. This implies that the formalism we describe in this section requires development of approximations to the functional E_{HXC}. Standard density functional approximations, however, can still be employed as starting points to develop new functionals.

Alternatively, instead of searching for more robust functionals, one can apply conventional functionals and find auxiliary functionals, e.g., scissor operators, that correct quantities that are crucial in the computational methodology and are underestimated by conventional XC functionals, such as subsystem ionization and affinity potentials, HOMO-LUMO gaps, etc.

B. Simplified formalism based on single-particle reference Hamiltonians

A simpler alternative to the formalism discussed above consists of employing single particle subsystem KS Hamiltonians to redefine the additive energy operator. Suppose we are given the solution to the multiplet problem of the isolated subsystems. Therefore, the orbitals used to construct the different degenerate Slater determinants are eigenfunctions of their corresponding subsystem KS Hamiltonian. This implies that a self-consistent field (SCF) procedure was solved. We denote the KS Hamiltonians of the subsystems as $\{\hat{h}_{\mathrm{s},Y}\}$. The form of the single-particle Hamiltonian depends on the symmetries of the isolated fragments. For example, for subsystems that upon isolation only feature a singlet or doublet symmetry, the following KS Hamiltonian can be assigned to them:

$$\hat{h}_{\mathrm{s},Y} = \hat{T}_Y + \int d^3\mathbf{r}[u_{\mathrm{HXC},Y}(\mathbf{r}) + v_Y(\mathbf{r})]\hat{\rho}_Y(\mathbf{r}). \tag{43}$$

For more general cases, e.g., those involving orbital degeneracies, the single-particle Hamiltonian may take the form $\hat{h}_{\mathrm{s},Y} = \sum_{ij\sigma\tau}\epsilon_{ij\sigma\tau,Y}\hat{a}^\dagger_{i\sigma,Y}\hat{a}_{j\tau,Y}$, where the indices i, j label occupied orbitals, and σ, τ the z-spin states. The matrix element $\epsilon_{ij\sigma\tau,Y}$ is determined by the expansion in terms of Slater determinants, the orbital orthonormal basis, and the XC potential. Now we define the single-particle additive energy operator as

$$\hat{\mathcal{H}}_{\mathrm{s},+} = \sum_Y \hat{h}_{\mathrm{s},Y}. \tag{44}$$

Similarly to the manner in previous sections, to this operator we can associate (i) an additive energy functional

$$E_{\mathrm{s},+}[\rho] = \min_{\eta\to\rho}(\min_{\bar{\Psi}\to\eta}\langle\bar{\Psi}|\hat{\mathcal{H}}_{\mathrm{s},+}|\bar{\Psi}\rangle) \tag{45}$$

[here the minimization is performed similarly to what was done in Eqs. (27) and (28), the difference being the type of additive energy operator]; (ii) a coupling energy functional

$$B_{\mathrm{s}}[\rho] = E_v[\rho] - E_{\mathrm{s},+}[\rho]; \tag{46}$$

and (iii) a coupling potential $\theta_{\mathrm{s}}(\mathbf{r})$ that follows a similar relation to that shown in Eq. (31). Note that for a given KS Hamiltonian $\hat{h}_{\mathrm{s},Y}$ there is a corresponding spectrum of noninteracting-particle wave functions $\{\Psi^Y_{\mathrm{s},\mathbf{I}_Y N_Y}\}$, such that $\hat{h}_{\mathrm{s},Y}|\Psi^Y_{\mathrm{s},\mathbf{I}_Y N_Y}\rangle = E^Y_{\mathrm{s},\mathbf{I}_Y N_Y}|\Psi^Y_{\mathrm{s},\mathbf{I}_Y N_Y}\rangle$. These wave functions can be used to express the auxiliary wave function $\bar{\Psi}$. Thus, constructing and performing computations with these KS wave functions is more tractable than with their fully correlated counterparts.

To select the reference energy operators one could use the Nagy formalism [32], and use equivalent weights $w_{\boldsymbol{\gamma}\boldsymbol{\gamma}'N'} = \delta_{N,N'}\delta_{\boldsymbol{\gamma},\boldsymbol{\gamma}'}/G$ where G is the total degeneracy of the reference system. For example, to describe a subsystem composed of a single atom, let N be number of electrons of the neutral state. We could take the neutral state as reference and solve the ensemble problem only using the KS potential for the neutral state and set $w_{\boldsymbol{\gamma}\boldsymbol{\gamma}N} = 1/G$ (the weights for states with number of electrons different than N would be zero), where G in this case would be the total degeneracy of the system (the number of spin configurations multiplied by the total angular momentum degeneracy).

C. Formalism based on energy functionals

The previous formulation demands minimization of the additive energy over the space spanned by all possible configurations of wave functions. In practice, however, one would solve the equations over a truncated space of auxiliary wave functions, as we pursued in Ref. [23]. It can be convenient, however, to relax coefficients and subsystem orbitals together, thereby limiting the number of needed configurations.

On the basis of Sec. IV A, we introduce an additive functional based on density matrices:

$$\mathcal{E}_+[\eta] = \min_{\bar{\Psi}_{\mathrm{s}}}\left\{\sum_Y E_Y[\hat{D}_{\mathrm{s},Y}](\mathbf{w}_Y)|\,\langle\bar{\Psi}_{\mathrm{s}}|\hat{\eta}(\mathbf{r})|\bar{\Psi}_{\mathrm{s}}\rangle = \eta(\mathbf{r})\right\}, \tag{47}$$

where we now consider auxiliary TP wave functions of the form

$$|\bar{\Psi}_{\mathrm{s}}\rangle = \sum_{N_1\mathbf{g}_1,\ldots,N_M\mathbf{g}_M,l_{\mathscr{S}}} C_{\mathrm{s},\mathbf{g}_1N_1,\ldots,\mathbf{g}_MN_M,l_{\mathscr{S}}}|\mathbf{g}_1N_1,\ldots,\mathbf{g}_MN_M;\mathscr{S},m_{\mathscr{S}},l_{\mathscr{S}}\rangle; \tag{48}$$

here we expanded the composite index $\boldsymbol{\gamma}_Y$ as $\boldsymbol{\gamma}_Y = \mathbf{g}_Y m_{S,Y}$; the vector $\mathbf{g}_Y$ specifies the degenerate state, its symmetry, and the spin symmetry (singlet, doublet, etc.). The spin-adapted ket reads

$$|\mathbf{g}_1N_1,\ldots,\mathbf{g}_MN_M;\mathscr{S},m_{\mathscr{S}},l_{\mathscr{S}}\rangle = \sum_{\mathcal{P}\{m_{S,1},\ldots,m_{S,M}\}} Q_{\mathcal{P}\{m_{S,1},\ldots,m_{S,M}\},l_{\mathscr{S}}}\left|\Psi^1_{\mathrm{s},\mathbf{g}_1\mathcal{P}m_{S,1}N_1}\right\rangle\cdots\left|\Psi^M_{\mathrm{s},\mathbf{g}_M\mathcal{P}m_{S,M}N_M}\right\rangle. \tag{49}$$

The auxiliary density matrix (DM) of the mth fragment is defined as

$$\hat{D}_{\mathrm{s},Y} = \sum_{N_Y\boldsymbol{\gamma}_Y\boldsymbol{\gamma}'_Y} w^Y_{\boldsymbol{\gamma}_Y\boldsymbol{\gamma}'_YN_Y}\left|\Psi^Y_{\mathrm{s},\boldsymbol{\gamma}_YN_Y}\right\rangle\left\langle\Psi^Y_{\mathrm{s},\boldsymbol{\gamma}'_YN_Y}\right|, \tag{50}$$

where

$$w^Y_{\boldsymbol{\gamma}_Y\boldsymbol{\gamma}'_YN_Y} = \mathrm{tr}_{X\neq Y}\left\{\left(\Psi^Y_{\mathrm{s},\boldsymbol{\gamma}_YN_Y}|\bar{\Psi}_{\mathrm{s}}\rangle\langle\bar{\Psi}_{\mathrm{s}}|\Psi^Y_{\mathrm{s},\boldsymbol{\gamma}'_YN_Y}\right)\right\}. \tag{51}$$

The above DM is a function of the matrices $\mathbf{w}^Y$. To minimize the sum of energies shown on the rhs of Eq. (47), the coefficients and the orbitals used to construct the wave functions $\{\Psi^Y_{\mathrm{s},\mathbf{J}_YN_Y}\}$ are the variational parameters. The density-matrix functional

E_Y reads

$$E_Y[\hat{D}_{\mathrm{s},Y}](\mathbf{w}_Y) = \mathrm{tr}\left\{\left[\hat{T}_Y + \int d^3\mathbf{r} v_Y(\mathbf{r})\hat{\rho}_Y(\mathbf{r})\right]\hat{D}_{\mathrm{s},Y}\right\} + E_{\mathrm{HXC}}[\rho_Y](\mathbf{w}_Y). \tag{52}$$

In this equation the density ρ_Y is expressed in terms of $\hat{D}_{\mathrm{s},Y}$ as

$$\rho_Y(\mathbf{r}) = \mathrm{tr}\{\hat{D}_{\mathrm{s},Y}\hat{\rho}_Y(\mathbf{r})\}. \tag{53}$$

This density is also a function of the matrix $\mathbf{w}^Y$ and the KS wave functions.

The minimization of the rhs of Eq. (47) can be accomplished by finding the minimum of the potential functional:

$$\mathcal{E}[\bar{\Psi}_\mathrm{s};\theta] = \sum_Y E_Y[\hat{D}_{\mathrm{s},Y}](\mathbf{w}_Y) + \int d^3\mathbf{r}\theta(\mathbf{r})\langle\bar{\Psi}_\mathrm{s}|\hat{\eta}(\mathbf{r})|\bar{\Psi}_\mathrm{s}\rangle. \tag{54}$$

In terms of noninteracting-particle wave functions, the above energy can be expressed as

$$\mathcal{E}[\bar{\Psi}_\mathrm{s};\theta] = \sum_Y \left\{\left[\sum_{N_Y\boldsymbol{\gamma}_Y\boldsymbol{\gamma}'_Y} w^Y_{\boldsymbol{\gamma}_Y\boldsymbol{\gamma}'_Y N_Y}\left\langle\Psi^Y_{\mathrm{s},\boldsymbol{\gamma}'_Y N_Y}\middle|\hat{T}_Y + \int d^3\mathbf{r}[v_Y(\mathbf{r}) + \theta(\mathbf{r})]\hat{\rho}_Y(\mathbf{r})\middle|\Psi^Y_{\mathrm{s},\boldsymbol{\gamma}_Y N_Y}\right\rangle\right] + E_{\mathrm{HXC}}[\rho_Y]\right\} \tag{55}$$

$$+ \sum_{\substack{Y N_Y\boldsymbol{\gamma}_Y\boldsymbol{\gamma}'_Y \\ X N_X\boldsymbol{\gamma}_X\boldsymbol{\gamma}'_X \\ Y\neq X}} L^{Y\boldsymbol{\gamma}_Y\boldsymbol{\gamma}'_Y N_Y}_{X\boldsymbol{\gamma}_X\boldsymbol{\gamma}'_X N_X}\int d^3\mathbf{r} f^Y_{\boldsymbol{\gamma}_Y\boldsymbol{\gamma}'_Y N_Y}(\mathbf{r})\theta(\mathbf{r})g^X_{\boldsymbol{\gamma}_X\boldsymbol{\gamma}'_X N_X}(\mathbf{r}),$$

where f and g are Dyson orbitals:

$$\begin{aligned} f^Y_{\boldsymbol{\gamma}_Y\boldsymbol{\gamma}'_Y N_Y}(\mathbf{r}) &= \left\langle\Psi^Y_{\mathrm{s},\boldsymbol{\gamma}'_Y N_Y+1}\middle|\hat{\psi}^\dagger_Y(\mathbf{r})\middle|\Psi^Y_{\mathrm{s},\boldsymbol{\gamma}_Y N_Y}\right\rangle, \\ g^X_{\boldsymbol{\gamma}_X\boldsymbol{\gamma}'_X N_X}(\mathbf{r}) &= \left\langle\Psi^X_{\mathrm{s},\boldsymbol{\gamma}'_X N_X-1}\middle|\hat{\psi}_X(\mathbf{r})\middle|\Psi^X_{\mathrm{s},\boldsymbol{\gamma}_X N_X}\right\rangle. \end{aligned} \tag{56}$$

For a given pair of fragments X and Y, the components of the tensor L are obtained by tracing out the degrees of freedom of all the fragments different from X and Y:

$$\begin{aligned} L^{Y\boldsymbol{\gamma}_Y\boldsymbol{\gamma}'_Y N_Y}_{X\boldsymbol{\gamma}_X\boldsymbol{\gamma}'_X N_X} &= \lambda_{YX}\mathrm{tr}_\mathrm{B}\left\{\left(\Psi^X_{\mathrm{s},\boldsymbol{\gamma}_X N_X}\middle|\left(\Psi^Y_{\mathrm{s},\boldsymbol{\gamma}_Y N_Y}\middle|\bar{\Psi}_\mathrm{s}\right\rangle\right.\right. \\ &\quad\left.\left.\times\left\langle\bar{\Psi}_\mathrm{s}\middle|\Psi^X_{\mathrm{s},\boldsymbol{\gamma}'_X N_X-1}\right\rangle\right)\middle|\Psi^Y_{\mathrm{s},\boldsymbol{\gamma}'_Y N_Y+1}\right)\right\}. \end{aligned} \tag{57}$$

Now we introduce the operator $\hat{\theta} = \int d^3\mathbf{r}\delta(\mathbf{r}-\hat{\mathbf{r}})\theta(\mathbf{r})$ ($\hat{\mathbf{r}}$ is the position operator) and the single-particle Hamiltonian

$$\hat{h}_Y[\theta] = \hat{T}_Y + \int d^3\mathbf{r}\left[v_Y(\mathbf{r}) + \theta(\mathbf{r}) + \frac{\delta E_{\mathrm{HXC}}}{\delta\rho_Y(\mathbf{r})}\right]\hat{\rho}_Y(\mathbf{r}). \tag{58}$$

The specific eigenvalue problem that results from minimizing Eq. (55) depends on the expansion of the wave functions $\{\Psi^Y_{\mathrm{s},\boldsymbol{\gamma}_Y N_Y}\}$ in terms of Slater determinants. But, in general, the minimization of Eq. (55) with respect to the orbitals leads to an eigenvalue problem of the form

$$\begin{aligned} &\sum_j p_{ij,Y}\hat{h}_Y[\theta]|\varphi_{j,Y}\rangle + \sum_{kX,\,X\neq Y} l_{ik,YX}\hat{\theta}|\varphi_{k,X}\rangle \\ &\quad = \sum_j p_{i,Y}\lambda_{ij,Y}|\varphi_{j,Y}\rangle, \end{aligned} \tag{59}$$

where $\{\lambda_{ij,Y}\}$ are the eigenvalues, which arise from imposing orthonormality of orbitals of the same fragment, and $p_{i,Y} = \sum_k(p_{ik,Y} + p_{ki,Y})/2$ (this contraction is only introduced for convenience, to potentially avoid large oscillations in the values of $\lambda_{ij,Y}$; however, one can set $p_{i,Y} = 1$). In this single-particle representation, the fragment-dependent operators are no longer needed, so $\langle\varphi_{i,Y}|\hat{\theta}(\mathbf{r})|\varphi_{k,X}\rangle$ is equivalent to the weighted inner product $\int d^3\mathbf{r}\,\varphi^*_{i,Y}(\mathbf{r})\theta(\mathbf{r})\varphi_{k,X}(\mathbf{r})$. The matrices $\mathbf{p}$, $\mathbf{l}$, and $\boldsymbol{\lambda}$ are Hermitian. The particular values of the matrices $\mathbf{p}$ and $\mathbf{l}$ depend on the nature of the subsystems being modeled.

To derive the secular equation of the coefficients, one needs to expand the equation $\partial\mathcal{E}/\partial C^*_{\mathrm{s},\bar{\mathbf{J}}_\mathrm{s}} = EC_{\mathrm{s},\bar{\mathbf{J}}_\mathrm{s}}$, where the wave functions are held fixed, $\bar{\mathbf{J}}_\mathrm{s}$ is the collection of subindices $\mathbf{g}_1 N_1,\ldots,\mathbf{g}_M N_M, l_{\mathscr{S}}$, and E is the eigenvalue. This differentiation leads to an additional eigenvalue problem of the form $(\mathbf{H}+\boldsymbol{\Theta})\mathbf{C}_\mathrm{s} = E\mathbf{C}_\mathrm{s}$, where $\mathbf{H}$ includes the energies of the subsystems. Employing the definition of the HXC energy functional, we can write the following estimate that could be applied to perform self-consistent cycles (Appendix C): $\partial E_Y/\partial w^Y_{\boldsymbol{\gamma}_Y\boldsymbol{\gamma}_Y N_Y} \approx E^Y_{\boldsymbol{\gamma}_Y N_Y}[\Psi^Y_{\mathrm{s},\boldsymbol{\gamma}_Y N_Y}]$, where $E^Y_{\boldsymbol{\gamma}_Y N_Y}$ is an energy functional of the wave function $\Psi^Y_{\mathrm{s},\boldsymbol{\gamma}_Y N_Y}$. We can also take $\partial E_Y/\partial w^Y_{\boldsymbol{\gamma}'_Y\boldsymbol{\gamma}_Y N_Y} = 0$ for $\boldsymbol{\gamma}'\neq\boldsymbol{\gamma}$ (Appendix C). These approximations can then be used to construct the matrix $\mathbf{H}$ by means of the chain rule; the specific form of this matrix depends on the number of degenerate states to be considered.

The above minimization procedure assumes the coupling potential is given. To obtain this potential we need to introduce the additive and coupling functionals. As above in Sec. III C, the additive energy can be defined as

$$E_+[\rho] = \min_\eta\{\mathcal{E}_+[\eta]|\eta(\mathbf{r}) - \zeta_\mathrm{s}[\eta](\mathbf{r}) = \rho(\mathbf{r})\}, \tag{60}$$

where

$$\zeta_\mathrm{s}[\eta](\mathbf{r}) = \langle\bar{\Psi}_\mathrm{s}[\eta]|\hat{\zeta}(\mathbf{r})|\bar{\Psi}_\mathrm{s}[\eta]\rangle; \tag{61}$$

here $|\Psi_\mathrm{s}[\eta]\rangle$ is the ket that solves the minimization problem shown in Eq. (47). If we define the coupling functional as

$$B[\rho] = E_v[\rho] - E_+[\rho], \tag{62}$$

then θ (the Lagrange multiplier) can be expressed as in Eq. (31), with B^{MB} replaced by B and z by z_s.

There are several possibilities to estimate the functional derivative of ζ_s with respect to the density. For example, we can approximate the coupling potential as $\theta(\mathbf{r}) \approx \delta B/\delta\rho(\mathbf{r})$, the additive energy functional as $E_+ \approx \mathcal{E}_+$, and $\eta \approx \rho$. In the case where overlap is non-negligible, the term $\delta\zeta_s(\mathbf{r}')/\delta\rho(\mathbf{r})$ can be approximated as $\delta(\mathbf{r}-\mathbf{r}')\zeta_s(\mathbf{r}')/\rho(\mathbf{r})$. This leads to

$$\theta(\mathbf{r}) \approx \frac{1}{1+\zeta_s(\mathbf{r})/\rho(\mathbf{r})}\frac{\delta B}{\delta\rho(\mathbf{r})}. \tag{63}$$

For simplicity, this approximation can also be combined with $E_+ \approx \mathcal{E}_+$. Another additional approximation is to neglect ζ_s in the above equation and simply use $\theta(\mathbf{r}) \approx \delta B/\delta\rho(\mathbf{r})$.

An alternative DFT approach to the one discussed here could involve using the different KS potentials for different fragment states, for example assigning a potential to the neutral state and a different one to a cation state, etc. This pathway could avoid XC potential discontinuities, but at the expense of orthogonality (orbitals from different particle-number states may not be orthogonal), so the couplings could be much more expensive because different sets of orbitals would be used to construct different states. For this reason, it can be more convenient to employ the same set of orbitals to describe all the states (as considered in this work), but the derivative discontinuities need to be taken into account. Although conventional density functionals lack these discontinuities, they can be calculated using portions of exact exchange, self-energies, Green's functions, and/or some new methodology (for example, one based on machine learning).

D. Controlling the level of theory

The ensemble XC energy functional is a significant source of information. For example, if we calculate a derivative of the XC energy with respect to an element of the matrix $\mathbf{w}^Y$, we would note that this functional corrects the derivative of the KS energy and introduces the derivatives of the Levy functional. In practice, however, traditional XC approximations lack this kind of property. One can resort to using hybrid functionals and single-particle energies. Regularly, these energies can approximate fundamental gaps. To employ hybrids in our theory, we just need to replace the density matrix functional E_Y by

$$E_Y^{\mathrm{nL}}[\hat{D}_{s,Y}](\mathbf{w}_Y) = \mathrm{tr}\left\{\left[\hat{T}_Y + \lambda\hat{W}_Y + \int d^3\mathbf{r}\, v_Y(\mathbf{r})\hat{\rho}_Y(\mathbf{r})\right]\hat{D}_{s,Y}\right\} + E_{\mathrm{HXC}}^{\lambda}[\rho_Y](\mathbf{w}_Y). \tag{64}$$

In this case the average of $\hat{W}_Y$ contains a Coulomb and a Fock term, while $E_{\mathrm{HXC}}^{\lambda}$ accounts for the remaining portions of Hartree-exchange energy, and includes 100% correlation.

For accelerated calculations, tight-binding Hamiltonians may be suitable, or energy operators based on neglect of differential overlap, to describe the fragments. For example,

$$E_Y^{\mathrm{TB}}[\hat{D}_{s,Y}](\mathbf{w}_Y) = \mathrm{tr}\left\{\left[\sum_{\mu\nu\sigma} t_{\mu\nu,\sigma}^{Y}\hat{d}_{\mu\sigma,Y}^{\dagger}\hat{d}_{\nu\sigma,Y}\right]\hat{D}_{s,Y}\right\}, \tag{65}$$

where the indices μ, ν run over the localized orbitals, and $\hat{d}_{\mu\sigma,Y}^{\dagger}$ (or $\hat{d}_{\nu\sigma,Y}$) creates (annihilates) a localized orbital labeled μ (or ν), with spin σ, at the Yth fragment. Different density-matrix functionals may be used for different subsystems. This offers the possibility of treating some fragments with correlated wave function methods, or assigning strongly correlated functionals to regions or subsystems that need such functionals. Additionally, reference Hamiltonians could be applied to treat certain regions of the molecule as well, for example, an energy of the form $E_Y = \mathrm{tr}\{\hat{h}_{s,Y}\hat{D}_{s,Y}\}$. Treating some molecular regions in this manner differs from the formalism presented in the previous section because of the different auxiliary wave function domains (in the previous section we consider all possible configurations, whereas in this section we consider a limited number of configurations). To automize the process of theory-level assignment, an artificial intelligence method might be helpful, a topic of future work.

V. TIME-DEPENDENT APPROACH

In this section we describe the TD versions of the many-body formalism and the DFT-based approaches, which were discussed in Secs. III C, IV B, and IV C. Although we presented two DFT methodologies in Secs. IV B and IV C, here we introduce a single TDDFT-based formalism that can use as initial state any auxiliary wave function produced by either of these two ground-state methods, implying that the initial-state dependency of the potentials that are herein defined is quite relevant. We remark, however, that other initial states are possible, such as linear combinations of auxiliary wave functions.

The main goal of this section is to propose a set of equations, within the LCOS theory, that can lead to the computation of the time evolution of density-derivable molecular electronic properties. A positive advantage of a TD fragment-based approach is the possibility of simulating how an electron charge is transferred between subsystems. Taking the system A+B as an example, with A and B being donor and acceptor molecules, upon the application of an external field, with a TD LCOS model one could compute the coherent dynamics of the process $\mathrm{A}+\mathrm{B} \rightarrow \mathrm{A}^+ + \mathrm{B}^-$. The TD electron population of a fragment, for instance, would be computed by averaging the spatial integral of the fragment density operator with respect to the TD auxiliary wave function of the system, in a fashion similar to that shown in Eq. (37) (the number of coefficients depends on the size of the ansatz); we discuss this type of wave function in this section. On the other hand, for this A+B system, with the introduction of a bath as a third subsystem, one could study the effects of dissipation on the electron-transfer process.

In general, by solving a set of TD LCOS evolution equations, we can compute the density response to external perturbation and extract quantities such as transition frequencies and transition dipole elements, which are properties needed to calculate optical and Raman intensities, charge-transfer rates, etc.

A. Many-body formulation

The formulation of the many-body TD LCOS method is motivated by the eigenvalue problem shown in Eq. (32). As in standard quantum mechanics, a direct extension from the

ground-state domain to the TD regime is accomplished by replacing the eigenenergy with the operator $i\partial/\partial t$. This leads to the evolution equation for the auxiliary wave function, which represents the system driven by an auxiliary driving scalar field ($\theta_{\rm D}$):

$$i\frac{\partial}{\partial t}|\bar{\Psi}(t)\rangle = \left\{\hat{\mathcal{H}}_+(t) + \int d^3\mathbf{r}\theta_{\rm D}(\mathbf{r},t)\hat{\eta}(\mathbf{r})\right\}|\bar{\Psi}(t)\rangle. \quad (66)$$

This equation can be solved with an ansatz similar to that shown in Eq. (22), but with TD excitation coefficients $C_{\mathbf{J}_1 N_1,\ldots,\mathbf{J}_M N_M, l_{\mathscr{S}}}(t)$. If the nuclear positions are functions of time, one may introduce a TD basis $\{\Psi^Y_{\mathbf{I}_Y N_Y}(\{\mathbf{R}_n(t)\})\}$, where $[\hat{H}_Y(t) - E^Y_{\mathbf{I}_Y N_Y}(t)]|\Psi^Y_{\mathbf{I}_Y N_Y}(\{\mathbf{R}_n(t)\})\rangle = 0$. The simplest TD problem one can derive from the above evolution equation is a TD 2×2 propagation—for example, by replacing $\mathcal{E}$ with $i\partial/\partial t$ in Eq. (36), and keeping the matrix on the left-hand side frozen. For a given initial state of the coefficients $C_{\rm N}$, $C_{\rm CT}$, solving the TD 2×2 problem would tell us how these coefficients evolve as functions of time, and indicate the TD behavior of the atomic charges.

As we show in Appendix D, the TD additive density $[\rho_+(\mathbf{r},t) = \langle\bar{\Psi}(t)|\hat{\rho}_+(\mathbf{r})|\bar{\Psi}(t)\rangle]$ and current density $[\mathbf{j}_+(\mathbf{r},t) = \langle\bar{\Psi}(t)|\hat{\mathbf{j}}_+(\mathbf{r})|\bar{\Psi}(t)\rangle]$ satisfy the evolution equations:

$$\begin{aligned}\frac{\partial\rho_+}{\partial t}(\mathbf{r},t) &= -\nabla\cdot\mathbf{j}_+(\mathbf{r},t),\\ \frac{\partial\mathbf{j}_+}{\partial t}(\mathbf{r},t) &= \mathbf{q}_+(\mathbf{r},t) - \eta(\mathbf{r},t)\nabla\theta_{\rm D}(\mathbf{r},t),\end{aligned} \quad (67)$$

where $\mathbf{q}_+$ is a force density term:

$$\mathbf{q}_+(\mathbf{r},t) = -i\langle\bar{\Psi}(t)|[\hat{\mathbf{j}}_+(\mathbf{r}),\hat{\mathcal{H}}_+(t)]|\bar{\Psi}(t)\rangle. \quad (68)$$

The evolution equations display a form similar to that of their full quantum mechanical counterparts. Similarly to the manner in standard, formal TDDFT, we assume that the initial state of the system $[|\bar{\Psi}(t=0)\rangle]$ is given. Furthermore, the potential $\theta_{\rm D}$ determines the pseudodensity and the total density uniquely. To prove this result, it can be shown that as long as the force density $-\eta\nabla\theta_{\rm D}$ is different from zero (and meets very similar conditions to those discussed in Ref. [33]) and the internal force density $\mathbf{q}_+$ is retarded (in time) with respect to vector $-\eta\nabla\theta_{\rm D}$, the density will feature a nonzero response, implying that the density is uniquely determined by the TD potential $\theta_{\rm D}$ (there are cases where the conditions considered in Ref. [33] do not hold, but such potentials are usually unphysical). This one-to-one map between densities and auxiliary driving potentials allows us to introduce a functional such that, given the initial states, and the TD density, it associates with the TD density ρ_+ an auxiliary driving potential $\theta_{\rm D}$.

For a given driving potential $v_{\rm D}(\mathbf{r},t)$ [for example, a dipolar interaction with a laser field $v_{\rm D}(\mathbf{r},t) = \mathbf{r}\cdot\mathbf{E}(t)$], the density of the locally coupled subsystems and the density of the real molecule should be the same in theory $[\rho_+(\mathbf{r},t) = \rho(\mathbf{r},t)]$. The density of the real system reads $\rho(\mathbf{r},t) = \langle\Psi(t)|\hat{\rho}(\mathbf{r})|\Psi(t)\rangle$, where $|\Psi(t)\rangle = \exp[-i\int_0^t dt'\hat{H}(t')]|\Psi_0\rangle$, and the "true" Hamiltonian of the system is $\hat{H}(t) = \hat{T} + \hat{W} + \int d^3\mathbf{r}[v_0(\mathbf{r},t) + v_{\rm D}(\mathbf{r},t)]\hat{\rho}(\mathbf{r})$, where $v_0(\mathbf{r},t)$ is the electron-nuclei interaction.

Comparing the equations for $\partial^2\rho_+/\partial t^2$ and $\partial^2\rho/\partial t^2$, we obtain

$$\begin{aligned}&\nabla\cdot[\eta(\mathbf{r},t)\nabla\theta_{\rm D}(\mathbf{r},t)]\\ &\quad= \nabla\cdot[\rho(\mathbf{r},t)\nabla v_{\rm D}(\mathbf{r},t)] + \mathbf{q}_+(\mathbf{r},t) - \mathbf{q}(\mathbf{r},t),\end{aligned} \quad (69)$$

where

$$\mathbf{q}(\mathbf{r},t) = -i\langle\Psi(t)|[\hat{\mathbf{j}}(\mathbf{r}),\hat{H}_0(t)]|\Psi(t)\rangle, \quad (70)$$

and $\hat{H}_0(t) = \hat{T} + \hat{W} + \int d^3\mathbf{r}\, v_0(\mathbf{r},t)\hat{\rho}(\mathbf{r})$. The above comparison indicates that the potential $\theta_{\rm D}(\mathbf{r},t)$ has a contribution from the external driving field. We now introduce the TD coupling potential $\theta(\mathbf{r},t)$, such that we can express

$$\theta_{\rm D}(\mathbf{r},t) = \theta(\mathbf{r},t) + v_{\rm D}(\mathbf{r},t). \quad (71)$$

By inserting the above equation into Eq. (69), we note that Eq. (69) is simplified if we also neglect the term $\nabla\cdot[\zeta(\mathbf{r},t)\nabla v_{\rm D}(\mathbf{r},t)]$ [where $\zeta(\mathbf{r},t) = \langle\bar{\Psi}(t)|\hat{\zeta}(\mathbf{r})|\bar{\Psi}(t)\rangle$]. This decomposition of the auxiliary potential allows us to express the TD coupling potential θ as a functional of the density of the system $[\rho_+(\mathbf{r},t)]$, and, approximately, as an independent function of the external driving field. Thus θ plays an analogous role to the XC potential of standard TDDFT; in Sec. V C we briefly discuss approximating $\theta(\mathbf{r},t)$.

B. TDDFT-based framework

We now introduce the formalism in which the electronic density of each fragment is represented by a system of noninteracting electrons. For formalism development purposes, we assume that the density $[\rho(\mathbf{r},t)]$ of the true system is known, as well as the auxiliary driving potential required to represent this density by the fragmented MB system, $\theta_{\rm D}(\mathbf{r},t)$. This implies that the TD additive density $[\rho_+(\mathbf{r},t)]$ is equivalent to $\rho(\mathbf{r},t)$.

As a direct simplification of the TD MB formalism presented in the previous subsection, we define the evolution equation for the wave function of the auxiliary system of electrons as

$$\left\{\hat{\mathcal{H}}_{{\rm s},+}(t) + \int d^3\mathbf{r}\theta_{{\rm s,D}}(\mathbf{r},t)\hat{\eta}(\mathbf{r})\right\}|\bar{\Psi}_{\rm s}(t)\rangle = i\frac{\partial}{\partial t}|\bar{\Psi}_{\rm s}(t)\rangle, \quad (72)$$

where $\hat{\mathcal{H}}_{{\rm s},+}(t) = \sum_Y \hat{h}_{{\rm s},Y}(t)$ and

$$\hat{h}_{{\rm s},Y}(t) = \hat{T}_Y + \int d^3\mathbf{r}\, v_{{\rm s},Y}(\mathbf{r},t)\hat{\rho}_Y(\mathbf{r}); \quad (73)$$

here the KS potentials $\{v_{{\rm s},Y}\}$ are assumed to be given, but we show later how they can be calculated. We introduced a new auxiliary potential, $\theta_{\rm s,D}$. This potential ensures that the TD density of the auxiliary system is equivalent to $\rho(\mathbf{r},t)$.

To find the solution to the above relation, we can use the eigenfunctions of a reference Hamiltonian [for example, the ground-state additive KS Hamiltonian plus $\int d^3\mathbf{r}\theta(\mathbf{r})\hat{\eta}(\mathbf{r})$] and, in order to construct the auxiliary wave function ansatz, include all possible intramolecular (singles, doubles, etc.) and intermolecular charge-transfer excitations. The method of variation of parameters may be invoked to find the solution to the above equations. For example, defining $|\bar{\Psi}_{\rm s}(t)\rangle =$

$\sum_{\mathbf{J}} C_{\mathrm{s},\mathbf{J}}(t)|\mathbf{J}\rangle_{\mathrm{s}}$ (where $\{|\mathbf{J}\rangle_{\mathrm{s}}\}$ is constructed using noninteracting, orthogonal, subsystem Slater determinants), the stationarity principle leads to the evolution equation in matrix form: $i\dot{\mathbf{C}}_{\mathrm{s}}(t) = [\mathbf{H}_{\mathrm{s},+}(t) + \boldsymbol{\Theta}_{\mathrm{s,D}}(t)]\mathbf{C}_{\mathrm{s}}(t)$.

As in the ground-state formalism, the averages of fragment specific operators, such as $\hat{H}_{\mathrm{s},Y}$, can be expressed in terms of density matrices. For example, the density, current-density, and force-density terms of fragment Y can be expressed as

$$\rho_{\mathrm{s},Y}(\mathbf{r},t) = \mathrm{tr}\{\hat{\rho}_Y(\mathbf{r})\hat{D}_{\mathrm{s},Y}(t)\},\ \mathbf{j}_{\mathrm{s},Y}(\mathbf{r},t) = \mathrm{tr}\{\hat{\mathbf{j}}_Y(\mathbf{r})\hat{D}_{\mathrm{s},Y}(t)\},$$
$$\mathbf{q}_{\mathrm{s},Y}(\mathbf{r},t) = \frac{1}{i}\mathrm{tr}\{[\hat{\mathbf{j}}_Y(\mathbf{r}), \hat{H}_{\mathrm{s},Y}]\hat{D}_{\mathrm{s},Y}(t)\}, \tag{74}$$

where $\hat{D}_{\mathrm{s},Y}(t) = \sum_{N_Y\mathbf{I}_Y\mathbf{I}'_Y} w^Y_{\mathbf{I}_Y\mathbf{I}'_Y N_Y}(t)|\Phi^Y_{\mathbf{I}_Y N_Y}\rangle\langle\Phi^Y_{\mathbf{I}'_Y N_Y}|$ and $\mathbf{w}^Y$ are calculated by tracing out bath states, as shown in Sec. IV C.

The motion equations of the total density and current density have similar forms to those for the correlated locally coupled subsystems:

$$\frac{\partial\rho_+}{\partial t}(\mathbf{r},t) = -\sum_Y \nabla\cdot\mathbf{j}_{\mathrm{s},Y}(\mathbf{r},t),$$
$$\frac{\partial\mathbf{j}_{\mathrm{s},+}}{\partial t}(\mathbf{r},t) = \sum_Y \mathbf{q}_{\mathrm{s},Y}(\mathbf{r},t) - \eta_{\mathrm{s}}(\mathbf{r},t)\nabla\theta_{\mathrm{s,D}}(\mathbf{r},t), \tag{75}$$

where $\eta_{\mathrm{s}}(\mathbf{r},t) = \langle\bar{\Psi}_{\mathrm{s}}(t)|\hat{\eta}(\mathbf{r})|\bar{\Psi}_{\mathrm{s}}(t)\rangle$. We use the same symbol (ρ_+) for the density because we want to define KS potentials in such a way that the additive densities of the many-body and auxiliary electron systems are the same. Comparing Eqs. (75) and (67), we can define the TD KS potential of a fragment as the solution of the Sturm-Liouville equation:

$$\nabla\cdot\rho_{\mathrm{s},Y}(\mathbf{r},t)\nabla v_{\mathrm{s},Y}(\mathbf{r},t)$$
$$= \nabla\cdot\Big[\rho_Y(\mathbf{r},t)\nabla v_Y(\mathbf{r},t) + \frac{1}{i}\mathrm{tr}\{[\hat{\mathbf{j}}_Y(\mathbf{r}), \hat{T}_Y]\hat{D}_{\mathrm{s},Y}(t)$$
$$- [\hat{\mathbf{j}}_Y(\mathbf{r}), \hat{T}_Y + \hat{W}_Y]\hat{D}_Y(t)\}\Big]. \tag{76}$$

The pseudodensities of both the MB and KS auxiliary systems are not strictly the same. Hence, as a formal condition, we demand that

$$\nabla\cdot\eta_{\mathrm{s}}(\mathbf{r},t)\nabla\theta_{\mathrm{s,D}}(\mathbf{r},t) = \nabla\cdot\eta(\mathbf{r},t)\nabla\theta_{\mathrm{D}}(\mathbf{r},t). \tag{77}$$

The above two equations represent relations that can be used to construct the KS potential for each fragment. Note that $v_{\mathrm{s},Y}$ depends on the initial states $D_{\mathrm{s},Y}(0)$ and $D_Y(0)$. In theory, constructing the Yth KS potential for all possible physical potentials leads to a map that depends on the auxiliary potential θ_{D}, which can be determined as a functional of the TD electronic density ρ_+. And, all the quantities shown in the above two equations, except $\{v_Y\}$, in principle could be given by maps that depend on θ_{D} (or ρ_+). For self-consistent calculations, however, a form for the HXC potential that depends on the Yth fragment density, or density matrix, can be convenient (as explored below).

Using the above matching procedure, we consider KS and coupling potentials as functionals of the total TD density of the system. In practice, the functionals discussed above could be approximated and one could solve the evolution equation of $|\bar{\Psi}_{\mathrm{s}}(t)\rangle$ *self-consistently* in order to determine the dynamic behavior of the total density of the system upon application of an external driving field.

Additional approximations can be considered, for example, the small overlap approximation in which $\zeta, \zeta_{\mathrm{s}} \ll \rho_+$, where $\zeta_{\mathrm{s}}(\mathbf{r},t) = \langle\bar{\Psi}_{\mathrm{s}}(t)|\hat{\zeta}(\mathbf{r})|\bar{\Psi}_{\mathrm{s}}(t)\rangle$. This allows us to write $\rho_{\mathrm{s},Y} \approx \rho_Y$, and by expressing $v_{\mathrm{s},Y}(\mathbf{r},t) = v_{\mathrm{HXC},Y}(\mathbf{r},t) + v_Y(\mathbf{r},t)$ we obtain

$$\nabla\cdot\rho_{\mathrm{s},Y}(\mathbf{r},t)\nabla v_{\mathrm{HXC},Y}(\mathbf{r},t)$$
$$\approx \nabla\cdot\Big[\frac{1}{i}\mathrm{tr}\{[\hat{\mathbf{j}}_Y(\mathbf{r}), \hat{T}_Y]\hat{D}_{\mathrm{s},Y}(t) - [\hat{\mathbf{j}}_Y(\mathbf{r}), \hat{T}_Y + \hat{W}_Y]\hat{D}_Y(t)\}\Big]. \tag{78}$$

This HXC functional can be taken as a functional of the electronic density of the Yth fragment and the matrix $\mathbf{w}_Y$ (Appendix E). However, because this type of functional has not been developed to date, one could employ, as a starting point, conventional functionals that only depend on the density of the Yth fragment—for example, invoking the LDA (local density approximation) XC potential determined by $\rho_Y(\mathbf{r},t)$, and assign such potential to fragment Y. Furthermore, $\eta_{\mathrm{s}} \approx \eta$ suggests that we can estimate the driving potential of the auxiliary system as

$$\theta_{\mathrm{s,D}}(\mathbf{r},t) \approx \theta_{\mathrm{D}}(\mathbf{r},t). \tag{79}$$

The above approximations let us express $\theta_{\mathrm{s,D}}(\mathbf{r},t) \approx \theta(\mathbf{r},t) + v_{\mathrm{D}}(\mathbf{r},t)$. This relation allows us to establish a connection with the ground-state formalisms described in Secs. IV B and IV C, which can be useful for applications of the present formalism.

C. Remarks on practical implementation of the TDDFT-based LCOS approach

To estimate the coupling potential, a starting point is its computation via functional derivation of the ground-state energy functional B^{MB}:

$$\theta(\mathbf{r},t) \approx \frac{\delta B^{\mathrm{MB}}}{\delta\rho(\mathbf{r})}\bigg|_{\rho(\mathbf{r})=\rho_+(\mathbf{r},t)}. \tag{80}$$

This approximation is local in time, and neglects dependency on how the density evolves between the initial propagation time and time t. One could also freeze the initial coupling potential and analyze the response to the external driving field; this approximation has shown benefits in the context of TD partition DFT [34].

Before performing propagations in practice, one first solves the ground-state problem (taken from Sec. IV B or IV C), generates the initial wave function $|\Psi_{\mathrm{s}}(t=0)\rangle$, and selects the approximations to the subsystem HXC and the coupling potentials; note that $\theta_{\mathrm{s,D}}(\mathbf{r},t) \approx \theta(\mathbf{r},t) + v_{\mathrm{D}}(\mathbf{r},t)$. Using these quantities, Eq. (72) can be solved and properties of interest (such as the TD molecular dipole) may be determined. Because the HXC and the coupling potentials are density functionals, similarly to what is done in the case of the standard TD KS equations, the propagation of $|\Psi_{\mathrm{s}}(t)\rangle$ must be performed in a self-consistent fashion.

The methodology we described in this subsection needs careful selection of subsystem HXC potentials so it can be connected with any of the two DFT approaches we described

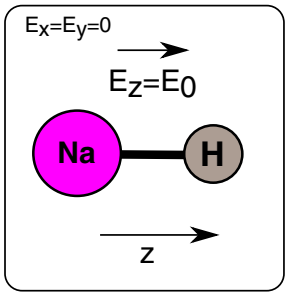

FIG. 2. Sodium hydride model, where a static electric field (E_0) is applied along the z direction.

in the previous section. For example, these two methodologies (from Secs. IV B and IV C) in general produce different ground-state auxiliary wave functions that can be taken as initial states for propagation. In this context, the initial-state dependence of the HXC and coupling potentials may have important roles that will need to be investigated in future work, and in numerical calculations.

Similarly to what we mentioned in Sec. III B, TD coupling potentials can also be generated using machine learning algorithms that can relate these potentials to variables such as the nuclear positions and external field parameters (such as laser frequency, intensity, and polarization). This route can serve as an alternative to potential DFT-based approaches.

VI. SIMPLE EXAMPLE FEATURING REFERENCE DFT ORBITALS AND TIME-DEPENDENT PROPAGATION

In this section, we examine the computation of the ground-state dissociation energy of sodium hydride (NaH) and its TD behavior upon the application of a static electric field (Fig. 2). We begin by considering the ground-state potential energy curve, based on the steps shown in Sec. III D. We model the molecule with two subsystems, one representing the sodium atom (subsystem A), and the other the hydrogen atom (subsystem B). We previously studied the ground state of LiH (Ref. [23]) and NaH (in the supplementary material of that paper) using Hartree-Fock references for the subsystem wave functions. Here we employ DFT wave functions instead. We refer to the method employed in Ref. [23] as the LCOS-HF method, and its slight variation considered in this work as the LCOS-LDA method. We continue employing atomic units throughout this section.

Formally, as in previous work, we use the functional $E_+[\rho]$ and the additive Hamiltonian $\hat{\mathcal{H}}_+ = \hat{H}_\mathrm{A} + \hat{H}_\mathrm{B}$. However, our LCOS-LDA application is quite close to employing the theory described in Sec. IV B, in which one would use an additive Hamiltonian of the form $\hat{\mathcal{H}}_{\mathrm{s},+} = \hat{h}_{\mathrm{s,A}} + \hat{h}_{\mathrm{s,B}}$, where $\hat{h}_{\mathrm{s},Y}$ ($Y = \mathrm{A}, \mathrm{B}$) represents the KS Hamiltonian of fragment Y. To implement an algorithm that uses this theory (Sec. IV B), and the operator $\hat{\mathcal{H}}_{\mathrm{s},+}$, we would need to develop a coupling functional. As a starting point one could consider the relation [which follows from the definitions of the functionals B_s and B^MB, Eqs. (46) and (29)]

$$B_\mathrm{s}[\rho] = B^\mathrm{MB}[\rho] + (E_+^\mathrm{MB}[\rho] - E_{\mathrm{s},+}[\rho]). \tag{81}$$

Hence, approximating the term in parentheses as an explicit density functional may facilitate developing a connection between these two coupling functionals.

First we run independent atomic KS calculations using the LDA functional (Slater+VWN-5 form). To obtain pure doublet atomic states for the neutral configuration, we employ spin-averaging of the atomic density matrices: The spin-up and spin-down valence s orbitals of Na and H are assigned occupations one half, and we compute the atomic ground states as restricted KS calculations. After completing the SCF procedures, we write the wave function expressed by Eq. (35) in terms of LDA orbitals, but with a slight modification: the valence s orbitals are now occupied by a single electron, so we can expand the neutral configuration to represent a molecular singlet as $1/\sqrt{2}(|\mathrm{A},\uparrow\rangle|\mathrm{B},\downarrow\rangle - |\mathrm{A},\downarrow\rangle|\mathrm{B},\uparrow\rangle)$. Using the LDA valence orbitals we compute the coupling potential and the elements required to construct the Hamiltonian matrix shown in Eq. (36), which is then diagonalized in a self-consistent fashion until differences in energy reach 1×10^{-6} [the quantity $I_\mathrm{A} - A_\mathrm{B}$ was taken from atomic, coupled-cluster singles and doubles (CCSD) calculations]. The coupling strength term is taken from previous work: $\lambda_\mathrm{AB} = 20\sqrt{2}$ (the $\sqrt{2}$ factor derives from the spin adaptation). The present calculations are performed within the PyQuante suite [35], and the 6-31G basis set.

The coupling functional for these calculations is expressed as follows: First, we write

$$B^\mathrm{MB} = B_\mathrm{k}^\mathrm{MB} + B_\mathrm{xc}^\mathrm{MB} + B_\mathrm{H,ext}^\mathrm{MB}, \tag{82}$$

where

$$B_\mathrm{H,ext}^\mathrm{MB}[\rho] = \langle\bar{\Psi}|\int d^3\mathbf{r}d^3\mathbf{r}'\frac{\hat{\rho}_\mathrm{A}(\mathbf{r})\hat{\rho}_\mathrm{B}(\mathbf{r}')}{|\mathbf{r}-\mathbf{r}'|} + \int d^3\mathbf{r}[\hat{\rho}_\mathrm{A}(\mathbf{r})v_\mathrm{B}(\mathbf{r}) + \hat{\rho}_\mathrm{B}(\mathbf{r})v_\mathrm{A}(\mathbf{r})]|\bar{\Psi}\rangle. \tag{83}$$

For the kinetic contribution we use

$$B_k^\mathrm{MB}[\rho] = C\int d^3\mathbf{r}\left[\rho^\alpha(\mathbf{r}) - \sum_{Y=\mathrm{A,B}}\tilde{\rho}_Y^\alpha(\mathbf{r})\right], \tag{84}$$

where C, α were determined in Ref. [23] as $C = 4.5$ and $\alpha = 2$. We apply the LDA to the XC portion of the functional B^MB:

$$B_\mathrm{xc}^\mathrm{MB}[\rho] = E_\mathrm{xc}^\mathrm{LDA}[\rho] - \sum_Y E_\mathrm{xc}^\mathrm{LDA}[\tilde{\rho}_Y]; \tag{85}$$

the densities $\{\tilde{\rho}_Y\}$ are functionals of the density, but during the self-consistent cycle they are simply taken as the averaged atomic densities, $\langle\bar{\Psi}|\hat{\rho}_Y(\mathbf{r})|\bar{\Psi}\rangle$ [the averaging is done similarly to the manner of Eq. (37)]. We note that the functional B^MB in combination with the LDA reference yields results quite similar to those of the calculations done with Hartree-Fock orbitals, Fig. 3. This implies that the binding curve is robust to relaxation effects introduced by the local KS potential, with respect to Hartree-Fock densities. This indicates some potential degree of functional transferability among references.

We now consider TD propagations under external fields. The molecular model is aligned with the z axis, and the origin is placed at the center of nuclear charge of the molecule with the hydrogen atom positioned on the positive half of the z axis.

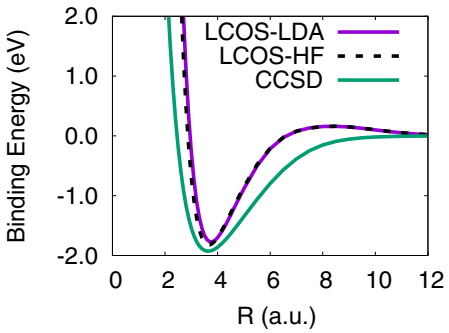

FIG. 3. Comparison between NaH binding energy curves determined by various techniques: LCOS-HF (as described in Ref. [23]), LCOS-LDA (studied in this work), and CCSD. R is the internuclear distance. The curves "LCOS-HF" and "CCSD" were adapted from Ref. [23].

For the TD evolution the internuclear distance is held fixed at 3.554 a.u., taken from an LDA (Slater+VWN-5) optimization with the basis set 6-31G* [36]. We employ the orbitals determined with LDA to propagate a simple 2×2 Hamiltonian matrix. In this matrix we only let the coupling potential evolve as a function of time and density. However, for calculations involving more states, propagation as described in Sec. V B could be more convenient.

These calculations follow the model discussed in Sec. V A, where the initial state is the ground state obtained in the previous LCOS calculations with LDA orbitals. The evolution equation that derives from Eq. (66) reads

$$\begin{pmatrix} \int d^3\mathbf{r}\theta_{\mathrm{D}}(\mathbf{r},t)\rho_{\mathrm{N}}(\mathbf{r}) & \Theta_{\mathrm{CT,N}}(t) \\ \Theta_{\mathrm{CT,N}}(t) & I_{\mathrm{A}} - A_{\mathrm{B}} + \int d^3\mathbf{r}\theta_{\mathrm{D}}(\mathbf{r},t)\rho_{\mathrm{CT}}(\mathbf{r}) \end{pmatrix} \times \begin{pmatrix} C_{\mathrm{N}}(t) \\ C_{\mathrm{CT}}(t) \end{pmatrix} = i\frac{d}{dt}\begin{pmatrix} C_{\mathrm{N}} \\ C_{\mathrm{CT}} \end{pmatrix}, \tag{86}$$

where θ_{D} is the sum of the coupling and the external potential, as shown in Eq. (71). The coupling potential is computed using the adiabatic approximation, Eq. (80). We thus express the auxiliary wave function of the system as

$$|\bar{\Psi}(t)\rangle = C_{\mathrm{N}}(t)|\mathrm{A,B}\rangle_{\mathcal{S}} + C_{\mathrm{CT}}(t)|\mathrm{A}^+\rangle|\mathrm{B}^-\rangle, \tag{87}$$

and quantities such as the average electron position and hydrogen electron population are determined with this wave function. Note that the Hamiltonian matrix is shifted by the additive energy of the neutral configuration; for this reason the term $I_{\mathrm{A}} - A_{\mathrm{B}}$ is present in the above equation (this shifting does not affect the computation of observables). The external potential describes the interaction between the dipole and an external, static electric field. Hence we express this potential simply as $v_{\mathrm{D}}(\mathbf{r},t) = zE_0$; the electric field is zero in the x and y directions. The off-diagonal coupling reads $\Theta_{\mathrm{CT,N}}(t) = (\lambda_{\mathrm{AB}}/\sqrt{2})\int d^3\mathbf{r}\theta_{\mathrm{D}}(\mathbf{r},t)\varphi_{\mathrm{HOMO,A}}(\mathbf{r})\varphi_{\mathrm{HOMO,B}}(\mathbf{r})$. The coupling strength λ_{AB} is the same used for the ground-state case.

The above equation was solved with the Crank-Nicolson method. For each step the Hamiltonian matrix is evaluated iteratively at the midstep until self-consistency is achieved (convergence criterion is 1×10^{-8} for the hydrogen occupation number). The calculations reported in Fig. 4 are based on 20 000 propagation steps in the range range $0 \leqslant t \leqslant 100$. For comparison we ran simulations with the TDDFT program Octopus [37]. These are TD-LDA calculations, but with the default functional, Slater exchange+Perdew-Zunger version of the LDA correlation energy and potential. The propagations were performed with the same number of steps and final time used for the TD-LCOS calculations, the spatial grid spacing is 0.2 a.u., and the simulation sphere radius is 8.0 a.u.

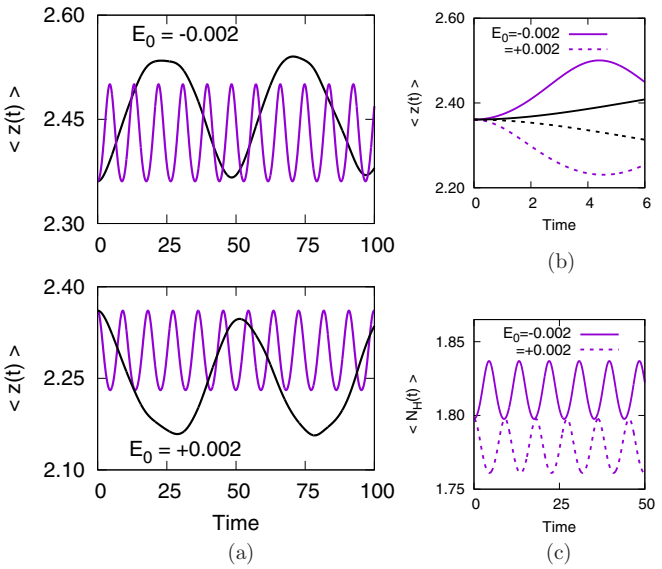

FIG. 4. (a) Computed average of the z component of the electronic position operator, in NaH, as a function of time. Upper subplot shows results for $E_0 = -0.002$, and bottom subplot for $E_0 = +0.002$. Purple lines: TD LCOS-LDA method; black line: TD LDA method (determined with Octopus). The TD LCOS-LDA curve is shifted to match the TD LDA line at $t = 0$ [we subtract 0.48 from the original TD LCOS-LDA data, $\langle z(t)\rangle$]. (b) Same as (a), but only displaying TD LCOS-LDA curves in the range $0 < t < 6$. (c) Hydrogen electron population [$\langle N_{\mathrm{H}}(t)\rangle$] as a function of time, as computed by our TD LCOS-LDA simplified model. Atomic units are implied.

We now consider the response of the ground state to two different static electric fields, $E_0 = -0.002$ and $+0.002$ (atomic units). The former field polarizes the molecule by transferring electron density to the hydrogen atom, whereas $E_0 = +0.002$ depolarizes the molecular electron density, by moving electron charge toward the sodium atom. Figure 4(a) shows the dependency of the average electronic position on time for $0 < t < 50$, and $E_0 = -0.002$ (top subplot) and $+0.002$ (bottom subplot); both subplots show the corresponding TD LCOS-LDA and TD LDA curves. The average position reads $\langle z(t)\rangle = \int d^3\mathbf{r}\, z\rho(\mathbf{r},t)$. In the top subplot we note that the molecule responds in a qualitatively correct fashion to the polarizing static field ($E_0 = -0.002$), by increasing the density polarization [recall that the z component of the TD dipole, $\mu_z(t)$, in this case is $-\langle z(t)\rangle$]. Although it displays amplitudes somewhat close to those computed with TD LDA, the function $\langle z(t)\rangle$ computed with TD LCOS-LDA (purple curve) oscillates with a higher frequency than in the TD LDA case (black curve). This discrepancy is caused by the high gap

(9.52 eV) between the two eigenvalues of the Hamiltonian matrix. In contrast, the first LDA (standard TDDFT, with basis set 6-31G*) linear-response excitation energy is 2.06 eV (the oscillation frequency of the real-time propagation should be close to the linear-response value, but it is not the same due to the extra relaxation induced by the TD XC potential). We expect that the high LCOS-LDA excitation energy can be improved by the addition of more configurations to the ansatz wave function, and the use of coupling functionals that are capable of lowering the zero-order transition frequencies via a linear-response analysis; this is further discussed in the next section. On the other hand, for the field $E_0 = -0.002$, we notice similar results, but with the field now depolarizing the molecule. Figure 4(c) shows the evolution of the hydrogen electron population, computed as $\langle\bar{\Psi}(t)|\int d^3\mathbf{r}\hat{\rho}_{\mathrm{B}}(\mathbf{r})|\bar{\Psi}(t)\rangle$. This figure indicates that the populations oscillate with a relatively small amplitude.

The considered TD ansatz, Eq. (87), neglects atomic density polarization, which would involve excitations from the valence s orbitals into orbitals with p and/or d character (not captured by the current model). In contrast, a more detailed expansion of the auxiliary wave function should include configurations in which one or more subsystems are excited, for example, $|\mathrm{A}^*\rangle|\mathrm{B}\rangle$, where $|\mathrm{A}^*\rangle$ has a valence orbital promoted to some virtual orbital. Another required configuration is $|\mathrm{A}^{+,*}\rangle|\mathrm{B}^-\rangle$, in which the cation A^+ is also excited. A larger wave function expansion can facilitate relaxation of the diagonal elements of the Hamiltonian matrix: The external field could stabilize subsystems with polarized densities, and the matrix propagation could give a dominant weight to the polarized configurations, leading to more accurate results.

VII. POTENTIAL APPLICATIONS OF THE TIME-DEPENDENT LCOS THEORY AND FUTURE PROSPECTS

In Sec. V we discussed a formalism to perform TD propagations of auxiliary wave functions. The theory requires a local coupling potential that can be determined using a density functional approximation. Initial applications of this theory, we believe, may encompass the computation of photoabsorption spectra within the linear response regime, the calculation of frequency-dependent electronic polarizability for processes that involve phonons such as in Raman spectroscopy, and coherent energy transfer.

For linear response calculations we can express the auxiliary wave function on the basis of singly excited states. To generate each of these states one starts from the ground state and excites a single electron from a valence state of a given fragment into an unoccupied state of the same fragment (this would be an intrafragment excitation), or excites that electron into a unoccupied state of a different one, which would entail an electron transfer excitation. Solution of the evolution equation for $|\bar{\Psi}_{\mathrm{s}}(t)\rangle$ in the linear regime and in the frequency space would lead to an eigenvalue problem that is quite similar to the Casida secular equation, which could be solved by methods based on Davidson algorithms. The frequencies obtained by solving the LCOS Casida equations could estimate the excitation frequencies of the real system, whereas the associated excitation vectors could be used to compute transition multipolar moments and related couplings to calculate coherent energy transfer rates.

For resonant Raman calculations one can apply an algorithm for accelerated computation of polarizabilities that could facilitate determining their gradients along normal-mode coordinates, as discussed in Refs. [38,39]. We expect the TD LCOS theory to offer ways to analyze in detail the effect of charge-transfer excitations on the polarizability response to vibrational motion, which could help in the assignment of experimental Raman bands. In addition, for the study of surface-enhanced Raman spectra, the TD LCOS approach might allow for controlling the level of theory needed to model the surface and plasmonic modes (if present). LCOS techniques may also be used to improve the accuracy of excitation energies associated with the transfer of an electron from/to the surface or nanoparticle (this is a topic that has been challenging for standard DFT methods [40,41]) and to reduce the amount of computing power required with respect to standard DFT-based methodologies.

Regarding future functional development, we believe there may be opportunities for integration of (TD) LCOS theories and methods with machine learning approaches. We note in the approximation used in the previous section that the coupling potential is dominant in regions with significant overlap between the subsystem electronic densities. In addition, the features of the coupling energy functional depend on the nature of the subsystems, such as their electron-nuclei potentials and their numbers of electrons. Assuming that the most important contributions to the coupling potential and energy originate mainly from the properties of the interface between subsystems, it could be feasible to design a machine learning algorithm that produces an approximation to the coupling energy functional, for example, by correlating descriptors of the interface with flexible functional forms that can be expressed using kernel methods, or with functional parameters, such as C and α (which were used in our modified Thomas-Fermi functional for the energy $B_{\mathrm{k}}^{\mathrm{MB}}$).

The theories and methods we have presented in this work are designed to feature three principal aspects: (i) controllability of computational scaling, so that one can select the level of theory desired to model each subsystem, ranging from orbital-free DFT up to high-level wave function theory; (ii) a Hamiltonian that includes a term that couples the fragments so energy and electrons can be transferred or exchanged; and (iii) the ability to satisfy size consistency when one or more fragments are placed at very large distances from the rest (which are assumed to be part of a conglomerate). To comply with point (i), we selected a coupling operator that includes a multiplicative potential where each of its values depends on a given point in space, and in time (for the case of propagating an auxiliary wave function). However, the potential can also depend nonlocally on the electronic density. This dependency is illustrated, for instance, by the Hartree potentials expressed in Eq. (83), which need integration over all space in order to give values at a single point. Refined kinetic and XC coupling energies may also display nonlocalities through approximations based on generalized density gradients, and beyond. In terms of time dependency, as with the XC potential of

standard TDDFT, the TD coupling potential may (preferably) depend on the history of the density, and the initial state of the system. Proper treatment of memory dependence has been suggested as a potential source for the improvement of computations in TDDFT [42,43], and this could be relevant in the context of TD-LCOS as well.

Our choice for the form of the interfragment coupling is not unique. Using a single coupling local potential is convenient for formalism development purposes and to establish a connection with a density functional. Nonetheless, other possibilities could be investigated (a few of them were briefly mentioned in Ref. [23], footnote 18), including combinations of different coupling terms. Operators that involve more than two fragments may bring benefits. For example, one can consider an operator of the form (which was not mentioned in Ref. [23]) $\psi_{\mathrm{A}}^{\dagger}(\mathbf{r})\psi_{\mathrm{B}}^{\dagger}(\mathbf{r})\psi_{\mathrm{C}}(\mathbf{r})\psi_{\mathrm{D}}(\mathbf{r})$, with C and D being two additional subsystems. Nonlocal interactions of the form $c(|\mathbf{r}'-\mathbf{r}|)\psi_{\mathrm{A}}^{\dagger}(\mathbf{r}')\psi_{\mathrm{A}}^{\dagger}(\mathbf{r})\psi_{\mathrm{B}}(\mathbf{r}')\psi_{\mathrm{B}}(\mathbf{r})$ could also be studied for future work, where c is a two-body coupling potential. For nonlocal interactions, a challenging aspect would be finding the relation between a coupling energy functional and its related two-body potential of interest. In addition, it could be possible to model fragment interaction with two different local potentials (β,ϑ) where one of them multiplies the additive density [$\beta(\mathbf{r})\hat{\rho}_{+}(\mathbf{r})$, for instance], and the other one multiplies the charge-transfer term: for example, $\vartheta(\mathbf{r})\sum_{Y\neq X}\hat{\tau}_{YX}(\mathbf{r})$. This quantity, ϑ, might replace the interaction matrix $\boldsymbol{\lambda}$ because it could control, locally, the strength of charge-transfer coupling between different subsystems. This decomposition may be convenient to control energy and charge transfer separately, but it might need two sources (perhaps two different energy functionals) to approximate the mentioned potentials.

VIII. CONCLUSION

We presented a set of formalisms based on the concept of molecular open subsystems that are locally coupled and can exchange electron charges and energy. These models employ auxiliary wave functions and Hamiltonians that can be used to develop simplified electronic-structure algorithms to determine quantities such as ground-state energies and densities, excited-state energies, electronic polarizabilities, and photoabsorption and photoemission spectra. The new methodologies depend on linear combinations of tensor products of subsystem wave functions, in which one can use fully correlated wave functions or Kohn-Sham Slater determinants. We presented approximations that may allow for integration with tools developed in other fragment-based formalisms such as subsystem, partition, and embedding DFTs.

Finally, we include here (Fig. 5) a schematic summary showing how the DFT-based theories may be applied in practice. The most important steps are the selection of a fragmentation scheme, approximations to the coupling energy, XC fragment potentials, the $\boldsymbol{\lambda}$ matrix, and the ansatz employed to solve the eigenvalue problem. Selecting the matrix $\boldsymbol{\lambda}$ is optional; one can set $\boldsymbol{\lambda}$ as the identity matrix and include terms in the coupling potential that account for the electron transfer processes.

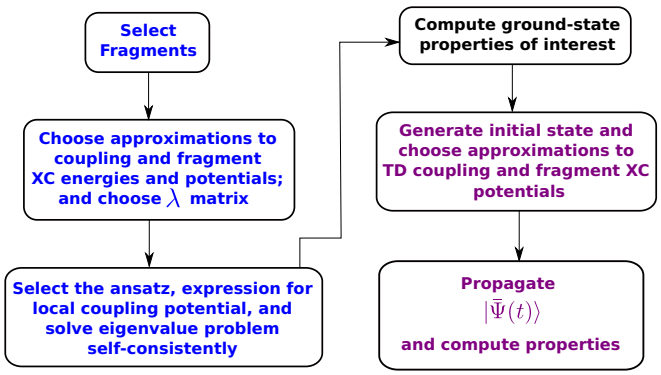

FIG. 5. Summary of the steps required to compute electronic properties with DFT-based LCOS methods. An additional implicit step is the selection of ground-state DFT formalism: the method based on reference Hamiltonians (Sec. IV B) or energy functionals (Sec. IV C).

ACKNOWLEDGMENTS

This work was supported by Department of Energy Grant No. DE-SC0004752 for theory, and by the Air Force Office of Scientific Research MURI (FA9550-14-1-0003) for applications.

APPENDIX A: TRACING OF STATES

For a state like

$$|\bar{\Psi}_{\mathrm{s}}\rangle = C_0\big|\Phi_{0,2}^{A}\big\rangle\big|\Phi_{0,1}^{B}\big\rangle + C_1\big|\Phi_{0,1}^{A}\big\rangle\big|\Phi_{1,2}^{B}\big\rangle + C_2\big|\Phi_{1,2}^{A}\big\rangle\big|\Phi_{0,1}^{B}\big\rangle, \tag{A1}$$

the projection $(\Phi_{0,2}^{A}|\bar{\Psi}_{\mathrm{s}}\rangle$ reads

$$\begin{aligned}\big(\Phi_{0,2}^{A}\big|\bar{\Psi}_{\mathrm{s}}\big\rangle &= C_0\big|\Phi_{0,1}^{B}\big\rangle,\\ \big(\Phi_{1,2}^{A}\big|\bar{\Psi}_{\mathrm{s}}\big\rangle &= C_2|\Phi_{0,1}^{B}\rangle,\end{aligned} \tag{A2}$$

and we have

$$w_{1,0;2}^{A} = C_2C_0^{*}\sum_{n}\big\langle\Phi_{n,1}^{B}\big|\Phi_{0,1}^{B}\big\rangle\big\langle\Phi_{0,1}^{B}\big|\Phi_{n,1}^{B}\big\rangle = C_2C_0^{*}, \tag{A3}$$

where $\{\Phi_{n,1}^{B}\}$ is an eigenbasis. Also note that $(\Phi_{0,2}^{A}|(\Phi_{0,1}^{B}|\bar{\Psi}\rangle = C_0$.

APPENDIX B: SPIN ADAPTATION

To construct an auxiliary wave function that obeys some additive spin symmetry, one could employ the Löwdin projection operators [44], or related techniques. For example,

$$\begin{aligned}\mathcal{O}_S &= \prod_{L\neq S}\frac{\hat{\boldsymbol{\mathcal{S}}}^2 - L(L+1)}{S(S+1)-L(L+1)},\\ \mathcal{O}'_{m_S} &= \prod_{\mu\neq m_S}\frac{\hat{\mathcal{S}}_z-\mu}{m_S-\mu}.\end{aligned} \tag{B1}$$

The product $\mathcal{O}'_{m_S}\mathcal{O}_S$ can thus be used to achieve the required spin eigenvalues. The application of these operators can transform an impure state into a configuration with the desired S

and m_S numbers. As an example, let us consider the auxiliary state (ignoring the core shells):

$$|\bar{\Psi}\rangle = |\phi_A\uparrow\psi_A\uparrow\rangle|\phi_B\downarrow\psi_B\downarrow\rangle. \tag{B2}$$

The first state is a Slater determinant assigned to subsystem A, in which the orbitals ϕ_A and ψ_A are occupied each with a spin-up electron. The second Slater determinant describes subsystem B. In this case, the orbitals ϕ_B and ψ_B are singly occupied with spin-down electrons.

We adapt $\bar{\Psi}$ as a singlet state. The corresponding projection operator is $\mathcal{O}_0 = 1/12(\hat{\boldsymbol{\mathcal{S}}}^4 - 8\hat{\boldsymbol{\mathcal{S}}}^2 + 12)$. The operation $\mathcal{O}_0|\bar{\Psi}\rangle$ can be carried out in terms of raising and lowering spin operators. For simplicity we express $|\phi_A\uparrow\psi_A\uparrow\rangle = |\uparrow\uparrow\rangle_A$, and $|\phi_B\downarrow\psi_B\downarrow\rangle = |\downarrow\downarrow\rangle_B$. The result is the following linear combination:

$$\begin{aligned}\mathcal{O}_0|\bar{\Psi}\rangle = \tfrac{1}{3}\big[&|\uparrow\uparrow\rangle_A|\downarrow\downarrow\rangle_B + |\downarrow\downarrow\rangle_A|\uparrow\uparrow\rangle_B - \tfrac{1}{2}(|\downarrow\uparrow\rangle_A|\uparrow\downarrow\rangle_B \\ &+ |\uparrow\downarrow\rangle_A|\downarrow\uparrow\rangle_B + |\downarrow\uparrow\rangle_A|\downarrow\uparrow\rangle_B + |\uparrow\downarrow\rangle_A|\uparrow\downarrow\rangle_B)\big],\end{aligned} \tag{B3}$$

which is a singlet state, with respect to the operator $\hat{\boldsymbol{\mathcal{S}}}^2$.

APPENDIX C: EXPRESSING THE DERIVATIVE $\partial E_Y/\partial w^Y_{\gamma_Y\gamma'_Y N_Y}$

For convenience we drop the superscript or subscript Y and write

$$E_0[\hat{D}_s](\mathbf{w}) = \mathrm{tr}\left\{\left[\hat{T} + \int d^3\mathbf{r}\, v(\mathbf{r})\hat{\rho}(\mathbf{r})\right]\hat{D}_s\right\} + E_{\mathrm{HXC}}[\rho](\mathbf{w}); \tag{C1}$$

the density ρ is expressed as

$$\rho(\mathbf{r}) = \mathrm{tr}\{\hat{D}_s\hat{\rho}(\mathbf{r})\}, \tag{C2}$$

where $\hat{D}_s = \sum_{\boldsymbol{\gamma}\boldsymbol{\gamma}'N} w_{\boldsymbol{\gamma}\boldsymbol{\gamma}'N}|\Psi_{s,\boldsymbol{\gamma}N}\rangle\langle\Psi_{s,\boldsymbol{\gamma}'N}|$, and $\{\Psi_{s,\boldsymbol{\gamma}N}\}$ are given combinations of Slater determinants with desired symmetries. Here we thus work within the standard quantum mechanical representation. First, note that we can express the functional $F[\rho](\mathbf{w})$ as follows:

$$F[\rho](\mathbf{w}) = \sum_{\boldsymbol{\gamma}\boldsymbol{\gamma}'N} w_{\boldsymbol{\gamma}\boldsymbol{\gamma}'N}\langle\tilde{\Psi}_{\boldsymbol{\gamma}'N}[\rho]|\hat{T} + \hat{W}|\tilde{\Psi}_{\boldsymbol{\gamma}N}[\rho]\rangle, \tag{C3}$$

where $\{\tilde{\Psi}_{\boldsymbol{\gamma}N}[\rho]\}$ are the wave functions that minimize the rhs of Eq. (38); these are functionals of the density ρ. Similarly, we express the functional $T_s[\rho](\mathbf{w})$ as

$$T_s[\rho](\mathbf{w}) = \sum_{\boldsymbol{\gamma}\boldsymbol{\gamma}'N} w_{\boldsymbol{\gamma}\boldsymbol{\gamma}'N}\langle\tilde{\Psi}_{s,\boldsymbol{\gamma}'N}[\rho]|\hat{T}|\tilde{\Psi}_{s,\boldsymbol{\gamma}N}[\rho]\rangle. \tag{C4}$$

Employing the definition of the HXC energy functional [Eq. (40)] we have that

$$\begin{aligned}E[\hat{D}_s](\mathbf{w}) = F[\rho](\mathbf{w}) &+ \int d^3\mathbf{r}\, v(\mathbf{r})\rho(\mathbf{r}) \\ &+ \mathrm{tr}\{\hat{D}_s\hat{T}\} - T_s[\rho](\mathbf{w}).\end{aligned} \tag{C5}$$

To compute the derivative of F with respect to $w_{\boldsymbol{\gamma}\boldsymbol{\gamma}'N}$, note that

$$\begin{aligned}\frac{\partial F}{\partial w_{\boldsymbol{\gamma}\boldsymbol{\gamma}'N}} = \lim_{\epsilon\to 0}\frac{1}{\epsilon}\{&F[\mathrm{tr}\{\hat{\rho}(\hat{D}_s + \epsilon|\Psi_{s,\boldsymbol{\gamma}N}\rangle\langle\Psi_{s,\boldsymbol{\gamma}'N}|)\}](\mathbf{w}') \\ &- F[\mathrm{tr}\{\hat{\rho}\hat{D}_s\}](\mathbf{w})\},\end{aligned} \tag{C6}$$

where $w'_{\boldsymbol{\gamma}\boldsymbol{\gamma}'N} = w_{\boldsymbol{\gamma}\boldsymbol{\gamma}'N} + \epsilon$, and all the remaining entries of $\mathbf{w}'$ equal those of $\mathbf{w}$. Invoking the set of wave functions $\{\tilde{\Psi}_{\boldsymbol{\gamma}_0N'}\}$ ($\boldsymbol{\gamma}_0N'$ are general indices) we obtain

$$\begin{aligned}\frac{\partial F}{\partial w_{\boldsymbol{\gamma}\boldsymbol{\gamma}'N}} = &\langle\tilde{\Psi}_{\boldsymbol{\gamma}'N}|\hat{T} + \hat{W}|\tilde{\Psi}_{\boldsymbol{\gamma}N}\rangle + \sum_{\boldsymbol{\gamma}_0\boldsymbol{\gamma}_1N'} w_{\boldsymbol{\gamma}_0\boldsymbol{\gamma}_1N'} \\ &\times\left(\left\langle\frac{\partial\tilde{\Psi}_{\boldsymbol{\gamma}_1N'}}{\partial w_{\boldsymbol{\gamma}\boldsymbol{\gamma}'N}}\middle|\hat{T} + \hat{W}\middle|\tilde{\Psi}_{\boldsymbol{\gamma}_0N'}\right\rangle + \mathrm{c.c.}\right).\end{aligned} \tag{C7}$$

A similar formula holds for the functional $T_s[\rho](\mathbf{w})$:

$$\begin{aligned}\frac{\partial T_s}{\partial w_{\boldsymbol{\gamma}\boldsymbol{\gamma}'N}} = &\langle\tilde{\Psi}_{s,\boldsymbol{\gamma}'N}|\hat{T}|\tilde{\Psi}_{s,\boldsymbol{\gamma}N}\rangle + \sum_{\boldsymbol{\gamma}_0\boldsymbol{\gamma}_1N'} w_{\boldsymbol{\gamma}_0\boldsymbol{\gamma}_1N'} \\ &\times\left(\left\langle\frac{\partial\tilde{\Psi}_{s,\boldsymbol{\gamma}_1N'}}{\partial w_{\boldsymbol{\gamma}\boldsymbol{\gamma}'N}}\middle|\hat{T}\middle|\tilde{\Psi}_{s,\boldsymbol{\gamma}_0N'}\right\rangle + \mathrm{c.c.}\right).\end{aligned} \tag{C8}$$

The derivatives of the wave functions $\{\tilde{\Psi}_{s,\boldsymbol{\gamma}_1N}, \tilde{\Psi}_{\boldsymbol{\gamma}_1N}\}$ can be calculated using perturbation theory. However, it may be computationally expensive to compute these terms. For the sake of simplicity we ignore these derivatives, and assume that the terms $\mathrm{tr}\{\hat{D}_s\hat{T}\} - T_s[\rho](\mathbf{w})$ cancel mutually. With these approximations we have that

$$\frac{\partial E}{\partial w_{\boldsymbol{\gamma}\boldsymbol{\gamma}'N}}[\hat{D}_s](\mathbf{w}) \approx \langle\tilde{\Psi}_{\boldsymbol{\gamma}'N}|\hat{T} + \hat{W} + \int d^3\mathbf{r}\hat{\rho}(\mathbf{r})v(\mathbf{r})|\tilde{\Psi}_{\boldsymbol{\gamma}N}\rangle. \tag{C9}$$

If the wave functions $\{\tilde{\Psi}_{\boldsymbol{\gamma}_0N'}\}$ are close to the eigenstates of the Hamiltonian $\hat{T} + \hat{W} + \int v\hat{\rho}$, then the derivative of $E[\hat{D}_s](\mathbf{w})$ with respect to weights with $\boldsymbol{\gamma} \neq \boldsymbol{\gamma}'$ can be neglected. Finally, for applications and the self-consistent cycle, one could estimate the element $\langle\tilde{\Psi}_{\boldsymbol{\gamma}N}|\hat{T} + \hat{W} + \int d^3\mathbf{r}\,\hat{\rho}(\mathbf{r})v(\mathbf{r})|\tilde{\Psi}_{\boldsymbol{\gamma}N}\rangle$ in terms of the KS analog of the wave function $\tilde{\Psi}_{\boldsymbol{\gamma}N}$, $\Psi_{s,\boldsymbol{\gamma}N}$ (where this is the wave function computed during the self-consistent cycle), perhaps by introducing an auxiliary density functional for this element that depends on $\Psi_{s,\boldsymbol{\gamma}N}$ and its electronic density.

APPENDIX D: TIME-DEPENDENT EQUATIONS FOR ADDITIVE DENSITIES AND CURRENTS

To prove the form of the evolution equations for the density and current density, Eq. (67), we start considering the

general equation:

$$i\frac{\partial}{\partial t}\langle\bar{\Psi}(t)|\hat{\Omega}(\mathbf{r})|\bar{\Psi}(t)\rangle = \langle\bar{\Psi}(t)|\left[\hat{\Omega}(\mathbf{r}), \hat{\mathcal{H}}'_+(t) + \sum_{Y\neq X}\lambda_{YX}\int d^3\mathbf{r}'\theta_{\rm D}(\mathbf{r}',t)\hat{\tau}_{YX}(\mathbf{r}')\right]|\bar{\Psi}(t)\rangle, \tag{D1}$$

where

$$\hat{\mathcal{H}}'_+(t) = \sum_X\left\{\hat{T}_X + \hat{W}_X + \int d^3\mathbf{r}'[v_X(\mathbf{r}',t)+\theta_{\rm D}(\mathbf{r}',t)]\hat{\rho}_X(\mathbf{r}')\right\} = \sum_X \hat{H}'_X(t); \tag{D2}$$

$\hat{\Omega}(\mathbf{r})$ is either the additive density operator $\hat{\rho}_+(\mathbf{r}) = \sum_X \hat{\rho}_X(\mathbf{r})$, or current $\hat{\mathbf{j}}_+(\mathbf{r}) = \sum_X \hat{\mathbf{j}}_X(\mathbf{r})$. The above relation follows from applying Eq. (72) to expand its left-hand-side term.

If we decompose the abstract operator, $\hat{\Omega}(\mathbf{r})$, in terms of fragment-specific components, $\hat{\Omega}(\mathbf{r}) = \sum_X \hat{\Omega}_X(\mathbf{r})$, then we have that

$$\begin{aligned} &i\frac{\partial}{\partial t}\langle\bar{\Psi}(t)|\hat{\Omega}(\mathbf{r})|\bar{\Psi}(t)\rangle \\ &\quad= \langle\bar{\Psi}(t)|\sum_X[\hat{\Omega}_X(\mathbf{r}), \hat{\mathcal{H}}'_X(t)] + \int d^3\mathbf{r}'\theta_{\rm D}(\mathbf{r}',t) \\ &\qquad\times\sum_{Y\neq X}\lambda_{YX}[\hat{\Omega}(\mathbf{r}), \hat{\tau}_{YX}(\mathbf{r}')]|\bar{\Psi}(t)\rangle. \end{aligned} \tag{D3}$$

The commutator $[\hat{\mathcal{H}}'_X(t), \hat{\Omega}_X(\mathbf{r})]$ is straightforward to evaluate for $\hat{\Omega}_X(\mathbf{r}) = \hat{\rho}_X(\mathbf{r})$ or $= \hat{\mathbf{j}}_X(\mathbf{r})$. It can be noted that the second commutator expression in the above relation can be written out as

$$\begin{aligned}[\hat{\Omega}(\mathbf{r}), \hat{\tau}_{YX}(\mathbf{r}')] &= [\hat{\Omega}_Y(\mathbf{r}), \hat{\psi}^\dagger_Y(\mathbf{r}')]\hat{\psi}_X(\mathbf{r}') \\ &\quad+ [\hat{\Omega}_X(\mathbf{r}), \hat{\psi}_X(\mathbf{r}')]\hat{\psi}^\dagger_Y(\mathbf{r}').\end{aligned} \tag{D4}$$

By using standard commutation rules we find the above result leads to

$$\int d^3\mathbf{r}'\theta_{\rm D}(\mathbf{r}')[\hat{\rho}_X(\mathbf{r}) + \hat{\rho}_Y(\mathbf{r}), \hat{\tau}_{YX}(\mathbf{r}')] = 0 \tag{D5}$$

and

$$\int d^3\mathbf{r}'\theta_{\rm D}(\mathbf{r}')[\hat{\mathbf{j}}_X(\mathbf{r}) + \hat{\mathbf{j}}_Y(\mathbf{r}), \hat{\tau}_{YX}(\mathbf{r}')] = \frac{1}{i}\nabla\theta_{\rm D}(\mathbf{r})\hat{\tau}_{YX}(\mathbf{r}). \tag{D6}$$

These last two expressions in combination with the calculation of the commutator $[\hat{\Omega}_X(\mathbf{r}), \hat{H}'_X(t)]$ indicate that the evolution equations for the additive density (ρ_+) and current density ($\mathbf{j}_+$) take the forms shown in Eq. (67).

APPENDIX E: TD HXC MAPS

There are different HXC maps that we can use for the self-consistent cycle. The most natural choice, based on the arguments above, is a map that depends on $\mathrm{tr}\{\hat{D}_{{\rm s},Y}\hat{\rho}_Y\}$. We can instead use a map that depends on the DM $\hat{D}_{{\rm s},Y}$ more generally. For a given set of fragment weights and auxiliary potential, the Yth KS potential determines the density of the system. We assume that $\hat{D}_Y$ can be expressed as a function of $\hat{D}_{{\rm s},Y}$:

$$\hat{D}_Y[\theta_{\rm D}](t) = \mathcal{F}(\hat{D}_{{\rm s},Y}[\theta_{\rm D}]). \tag{E1}$$

For self-consistent calculations, we can thus express an approximation to the HXC potential as a functional $v^{\rm I}_{{\rm HXC},Y}[\hat{D}_{{\rm s},Y}(t)]$,

$$\begin{aligned}&\nabla\cdot\rho_Y(\mathbf{r},t)\nabla v^{\rm I}_{{\rm HXC},Y}(\mathbf{r},t) \\ &\quad\approx \nabla\cdot\left(\frac{1}{i}\mathrm{tr}\{[\hat{\mathbf{j}}_Y(\mathbf{r}), \hat{T}_Y]\hat{D}_{{\rm s},Y}(t) \right. \\ &\qquad\left. - [\hat{\mathbf{j}}_Y(\mathbf{r}), \hat{T}_Y + \hat{W}_Y]\mathcal{F}(\hat{D}_{{\rm s},Y}(t))\}\right),\end{aligned} \tag{E2}$$

and for additional simplicity as a functional that depends only on the density ρ_Y, $\tilde{v}_{{\rm HXC},Y}[\rho_Y](\mathbf{r},t;\mathbf{w}_Y)$. The above equation can be considered to develop HXC potentials that depend on the weight matrix.

APPENDIX F: CONNECTION WITH PARTITION DENSITY FUNCTIONAL THEORY

If we replace the operator $\hat{\eta}(\mathbf{r})$ with $\hat{\rho}_+(\mathbf{r})$ and disregard the spin-adaption technique, the resulting formalism becomes partition density functional theory (PDFT) [27], in which the coupling potential would be the same as the partition potential. The interpretation, however, is different. In PDFT, the subsystems are isolated from one another and they exchange electrons with an external reservoir, where the system temperature is 0 K. Therefore, the state of a subsystem in PDFT can be given by an open-system density matrix, or the TP wave function of the whole collection of fragments can be expressed as a product of independent kets in Fock space.

[1] A. J. Cohen, P. Mori-Sánchez, and W. Yang, Science **321**, 792 (2008).

[2] J. P. Perdew, R. G. Parr, M. Levy, and J. L. Balduz, Jr., Phys. Rev. Lett. **49**, 1691 (1982).

[3] T. A. Wesolowski, S. Shedge, and X. Zhou, Chem. Rev. **115**, 5891 (2015).

[4] F. Libisch, C. Huang, and E. A. Carter, Acc. Chem. Res. **47**, 2768 (2014).

[5] C. Huang and E. A. Carter, J. Chem. Phys. **135**, 194104 (2011).

[6] G. Knizia and G. K.-L. Chan, Phys. Rev. Lett. **109**, 186404 (2012).

[7] S. Gómez, J. Nafziger, A. Restrepo, and A. Wasserman J. Chem. Phys. **146**, 074106 (2017).

[8] J. D. Goodpaster, T. A. Barnes, and T. F. Miller III, J. Chem. Phys. **134**, 164108 (2011).

[9] M. E. Casida and T. A. Wesołowski, Int. J. Quantum Chem. **96**, 577 (2004).

[10] J. Neugebauer, M. J. Louwerse, E. J. Baerends, and T. A. Wesolowski, J. Chem. Phys. **122**, 094115 (2005).

[11] M. Chiba, D. G. Fedorov, and K. Kitaura, J. Chem. Phys. **127**, 104108 (2007).

[12] G. Albareda, J. Suñé, and X. Oriols, Phys. Rev. B **79**, 075315 (2009).

[13] G. Fradelos, J. J. Lutz, T. A. Wesołowski, P. Piecuch, and M. Włoch, J. Chem. Theory Comput. **7**, 1647 (2011).

[14] J. Neugebauer, Phys. Rep. **489**, 1 (2010).

[15] A. S. P. Gomes and C. R. Jacob, Annu. Rep. Prog. Chem., Sect. C: Phys. Chem. **108**, 222 (2012).

[16] M. Pavanello, J. Chem. Phys. **138**, 204118 (2013).

[17] A. Krishtal, D. Sinha, A. Genova, and M. Pavanello, J. Phys.: Condens. Matter **27**, 183202 (2015).

[18] A. Krishtal and M. Pavanello, J. Chem. Phys. **144**, 124118 (2016).

[19] T. Zelovich, T. Hansen, Z.-F. Liu, J. B. Neaton, L. Kronik, and O. Hod, J. Chem. Phys. **146**, 092331 (2017).

[20] A. Genova, D. Ceresoli, A. Krishtal, O. Andreussi, R. A. DiStasio, and M. Pavanello, Int. J. Quantum Chem. **117**, e25401 (2017).

[21] P. Mori-Sánchez and A. J. Cohen, Phys. Chem. Chem. Phys. **16**, 14378 (2014).

[22] M. A. Mosquera and A. Wasserman, J. Chem. Theory Comput. **11**, 3530 (2015).

[23] M. A. Mosquera, M. A. Ratner, and G. C. Schatz, J. Chem. Phys. **149**, 034105 (2018).

[24] Using Pauli matrices this operator reads $\hat{\mathbf{S}}_Y = 1/2 \sum_{ss'} \int d^3\mathbf{r} \hat{\psi}^\dagger_{s,Y}(\mathbf{r}) \boldsymbol{\sigma}_{ss'} \hat{\psi}_{s',Y}(\mathbf{r})$, where $\boldsymbol{\sigma}$ is the Pauli spin-matrix vector, and the indices s, s' run over $\uparrow, \downarrow$.

[25] A possible, alternative formalism that could derive from our work would consist of employing the expectation value of $\hat{\mathcal{H}}$ as an approximation to the ground-state energy. In such case, the challenge would be finding ways to compute the local potential $\theta(\mathbf{r})$; in our LCOS theory this is accomplished by taking a derivative of a density functional (Secs. III C, IV B, and IV C).

[26] Note that $\langle \mathbf{J}_1 N_1, \ldots, \mathbf{J}_M N_M | \mathbf{J}'_1 N'_1, \ldots, \mathbf{J}'_M N'_M \rangle = \delta_{N_1 N'_1} \delta_{\mathbf{J}_1 \mathbf{J}'_1} \ldots \delta_{N_M N'_M} \delta_{\mathbf{J}_M \mathbf{J}'_M}$.

[27] P. Elliott, M. H. Cohen, A. Wasserman, and K. Burke, J. Chem. Theory Comput. **5**, 827 (2009).

[28] A. Pribram-Jones, P. E. Grabowski, and K. Burke, Phys. Rev. Lett. **116**, 233001 (2016).

[29] A. Pribram-Jones, Z.-h. Yang, J. R. Trail, K. Burke, R. J. Needs, and C. A. Ullrich, J. Chem. Phys. **140**, 18A541 (2014).

[30] J. C. Snyder, M. Rupp, K. Hansen, K.-R. Müller, and K. Burke, Phys. Rev. Lett. **108**, 253002 (2012).

[31] In contrast to Ref. [23], the off-diagonal coupling Θ_{CT} includes a $1/\sqrt{2}$ factor, which is absent in the secular equation derived in Ref. [23]. For applications to other systems, we expect this type of numerical factor to emerge in the secular equation because of the different normalization factors the spin-adapted configuration may feature and the algebraic properties of the operator $\zeta(\mathbf{r})$. By simply rescaling the interaction constant of the present spin-adapted example, $\lambda_{\mathrm{AB}} \to \sqrt{2}\lambda_{\mathrm{AB}}$, and by applying the values used in Ref. [23] for the rescaled interaction parameter, we obtain the same occupation numbers and binding energies as in Ref. [23].

[32] A. Nagy, Phys. Rev. A **57**, 1672 (1998).

[33] M. A. Mosquera, J. Chem. Phys. **147**, 134110 (2017).

[34] M. A. Mosquera, D. Jensen, and A. Wasserman, Phys. Rev. Lett. **111**, 023001 (2013).

[35] R. P. Muller, Python Quantum Chemistry (PyQuante) Program, http://pyquante.sourceforge.net.

[36] M. Valiev, E. J. Bylaska, N. Govind, K. Kowalski, T. P. Straatsma, H. J. Van Dam, D. Wang, J. Nieplocha, E. Apra, T. L. Windus *et al.*, Comput. Phys. Commun. **181**, 1477 (2010).

[37] X. Andrade, D. Strubbe, U. De Giovannini, A. H. Larsen, M. J. Oliveira, J. Alberdi-Rodriguez, A. Varas, I. Theophilou, N. Helbig, M. J. Verstraete *et al.*, Phys. Chem. Chem. Phys. **17**, 31371 (2015).

[38] L. Jensen, L. Zhao, J. Autschbach, and G. Schatz, J. Chem. Phys. **123**, 174110 (2005).

[39] L. Jensen, J. Autschbach, and G. C. Schatz, J. Chem. Phys. **122**, 224115 (2005).

[40] R. L. Gieseking, M. A. Ratner, and G. C. Schatz, Faraday Discuss. **205**, 149 (2017).

[41] J. E. Moore, S. M. Morton, and L. Jensen, J. Phys. Chem. Lett. **3**, 2470 (2012).

[42] N. T. Maitra, K. Burke, and C. Woodward, Phys. Rev. Lett. **89**, 023002 (2002).

[43] N. T. Maitra, Int. J. of Quantum Chem. **102**, 573 (2005).

[44] P.-O. Löwdin, Rev. Mod. Phys. **36**, 966 (1964).